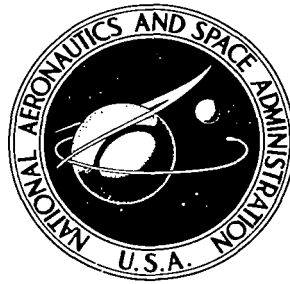


NASA TECHNICAL NOTE



NASA TN D-5728

c. 1

NASA TN D-5728



**LOAN COPY: RETURN TO
AFWL (WL0L)
KIRTLAND AFB, N MEX**

ACCURACY OF FINITE ELEMENT APPROXIMATIONS TO STRUCTURAL PROBLEMS

*by Joseph E. Walz, Robert E. Fulton, Nancy Jane Cyrus,
and Richard T. Eppink*

*Langley Research Center
Langley Station, Hampton, Va.*





0131532

1. Report No. NASA TN D-5728	2. Government Accession No.	3. Recipient's Catalog No.	
4. Title and Subtitle ACCURACY OF FINITE ELEMENT APPROXIMATIONS TO STRUCTURAL PROBLEMS		5. Report Date March 1970	
		6. Performing Organization Code	
7. Author(s) Joseph E. Walz, Robert E. Fulton, Nancy Jane Cyrus, and Richard T. Eppink		8. Performing Organization Report No. L-5656	
		10. Work Unit No. 126-14-16-03-23	
9. Performing Organization Name and Address NASA Langley Research Center Hampton, Va. 23365		11. Contract or Grant No.	
		13. Type of Report and Period Covered Technical Note	
12. Sponsoring Agency Name and Address National Aeronautics and Space Administration Washington, D.C. 20546		14. Sponsoring Agency Code	
		15. Supplementary Notes	
16. Abstract <p>This paper reports on a theoretical investigation of the convergence properties of several finite element approximations in current use and assesses the magnitude of the principal errors resulting from their use for certain classes of structural problems. The method is based on classical order of error analyses commonly used to evaluate finite difference methods. Through the use of Taylor series the differential or partial differential equations which represent the convergence and principal error characteristics of the finite element equations are found. These resulting equations are then compared with known equations governing the continuum and the error terms are evaluated for selected problems. Finite elements for bar, beam, plane stress, and plate bending problems are studied as well as the use of straight or curved elements to approximate curved beams. The results of the study provide basic information on the effect of interelement compatibility, unequal size elements, discrepancies in triangular element approximations, flat element approximations to curved structures, and the number of elements required for a desired degree of accuracy.</p>			
17. Key Words Suggested by Author(s) Finite element methods Structural analysis Numerical methods Error analysis		18. Distribution Statement Unclassified - Unlimited	
19. Security Classif. (of this report) Unclassified	20. Security Classif. (of this page) Unclassified	21. No. of Pages 53	22. Price* \$3.00

*For sale by the Clearinghouse for Federal Scientific and Technical Information
Springfield, Virginia 22151

ACCURACY OF FINITE ELEMENT APPROXIMATIONS TO STRUCTURAL PROBLEMS

By Joseph E. Walz, Robert E. Fulton, Nancy Jane Cyrus,
and Richard T. Eppink
Langley Research Center

SUMMARY

This paper reports on a theoretical investigation of the convergence properties of several finite element approximations in current use and assesses the magnitude of the principal errors resulting from their use for certain classes of structural problems. The method is based on classical order of error analyses commonly used to evaluate finite difference methods. Through the use of Taylor series the differential or partial differential equations which represent the convergence and principal error characteristics of the finite element equations are found. These resulting equations are then compared with known equations governing the continuum and the error terms are evaluated for selected problems. Finite elements for bar, beam, plane stress, and plate bending problems are studied as well as the use of straight or curved elements to approximate curved beams. The results of the study provide basic information on the effect of inter-element compatibility, unequal size elements, discrepancies in triangular element approximations, flat element approximations to curved structures, and the number of elements required for a desired degree of accuracy.

INTRODUCTION

Finite element methods have been used for many years with good success in the analyses of complex structures and many aerospace structures are designed on the basis of these analyses. Although the use of these methods is widespread, not enough is known of the theoretical accuracy and convergence properties of finite element models when used to represent structures. Accuracy studies are usually based on numerical solutions to specific problems for comparison with known results. Convergence studies are carried out by investigating the convergence of the numerical results as the number of elements is increased. (See ref. 1, for example.) Such methods, while valuable in providing a cursory assessment of the adequacy of various model approximations, are heavily dependent on the numerical data and the problem studied and may obscure the true

character of the approximation. More basic information is needed on the accuracy and convergence properties of various finite elements for structural approximations.

The purpose of the present paper is to report on an analytical investigation of the accuracy of several finite element stiffness method approximations in current use and to assess the magnitude of the errors resulting from the use of these approximations for certain classes of structural problems. The present paper includes results which were summarized in references 2 and 3 and in addition provides a comprehensive explanation of the background details of the error analysis procedure which led to these results. The method used is based on classical order of error analyses commonly used to evaluate the discretization errors of finite difference methods. Through the use of Taylor series the ordinary or partial differential equations are found from which the convergence and error characteristics of the finite element equations can be determined. These resulting equations are compared with the known continuum equations governing the structure. The discretization error in the finite element approximation is evaluated for a limited class of deflection and vibration problems to provide simple formulas for the size of an element required to obtain a certain degree of accuracy. (See refs. 4 and 5.) Finite elements for bar, beam, plane stress, and plate bending problems are studied as well as the use of straight and curved elements to approximate a curved beam.

SYMBOLS

A	cross-sectional area of one-dimensional element
a, b	length of rectangular panel in x- and y-directions, respectively
B	extensional stiffness of plate, $\frac{Et}{1 - \mu^2}$
c	constant
D	bending stiffness of plate, $\frac{Et^3}{12(1 - \mu^2)}$
E	Young's modulus
F	finite element nodal force
F_x, F_y	nodal force in x- and y-directions, respectively, of plane stress element
h	reference length of finite element

I	moment of inertia of cross section
i, j	i, j th grid point
$[K]$	element stiffness matrix
L	length of one-dimensional structure
M_x, M_y	bending moments in x- and y-directions, respectively (see fig. 7)
m, n	harmonic wave numbers for sinusoidally distributed loads
\bar{m}	mass per unit length for one-dimensional element; mass per unit area for two-dimensional element
N	number of elements per harmonic wave number, $\frac{a}{hm}$ or $\frac{L}{hm}$
$O(h)$	omitted discretization error term of order h
p	tangential loading on bar and arch structures
p_0	amplitude of sinusoidal tangential or inplane loading
p_x, p_y	distributed inplane loading in x- and y-directions, respectively
q	transverse loading
\bar{q}	magnitude of uniform pressure
q_0	amplitude of sinusoidally distributed transverse loading
R	radius of arch
t	thickness of plate
u, v, w	displacements in x-, y-, and z-directions, respectively
u_0	amplitude of sinusoidally varying displacement

x, y, z	rectangular coordinates
α	constant indicating ratio of element dimensions
$\{\delta\}$	vector of nodal displacements
ϵ	discretization error in displacement or frequency parameter
ϵ_1, ϵ_2	discretization errors in displacement and frequency parameters, respectively, for plate bending examples
$\epsilon_u, \epsilon_v, \epsilon_w$	discretization errors in displacements u , v , and w , respectively
θ, φ	nodal rotation variables for bending element about y - and x -axes, respectively
μ	Poisson's ratio
ρ	radius of gyration of cross section
$\sigma_x, \sigma_y, \tau_{xy}$	normal stresses in x - and y -directions and shear stress, respectively
ω	circular frequency

Subscripts:

ex	exact
i	identification for i th grid point

Abbreviation:

ACM	Adini, Clough, and Melosh plate bending model
-----	---

Prime or Roman numeral with a symbol denotes differentiation with respect to x .

Subscript following a comma denotes differentiation with respect to the indicated variable.

ERROR ANALYSIS PROCEDURE

Two main sources of error result from the use of finite element methods to solve structural problems. These may be conveniently separated into round-off error and discretization error. Round-off error is that error associated with the accuracy with which numbers are manipulated in a computer and is not considered in the present paper. Discretization error is that error associated with using discrete variables to represent a problem where the state variables are continuous. This error occurs irrespective of the accuracy of numerical calculations and occurs in structural problems when finite elements are used to approximate a continuous structure. Discretization errors may be of two kinds, as follows: (1) Errors which are a function of the size of the element and which vanish as the element size vanishes; and (2) errors which do not vanish when the element size vanishes. The relative merit of elements and/or patterns which lead to the first kind of discretization errors depends on the relative rate at which the error vanishes with element size. Elements and/or patterns which lead to the second kind of discretization errors are unsatisfactory approximations and should be recognized and avoided. The present paper deals with an assessment of both kinds of discretization errors in finite element approximations.

The method used in the study is to obtain the typical finite element equations which express force equilibrium at a reference node point in terms of displacement variables. These finite element equations (which are a class of difference equations) are then expanded in Taylor series about the nodal point to obtain the differential equations equivalent to the finite element equations at that node. The resulting differential equations are compared with the governing equations for the continuum approximated. A simple bar element approximation is treated in detail as an example to characterize the method and to define the terms to be used in the study.

Example Discretization Error Analysis

The force-displacement relations of a typical one-dimensional structural element having ends $i - 1$ and i are

$$\begin{Bmatrix} \{F_{i-1}\} \\ \{F_i\} \end{Bmatrix} = [K] \begin{Bmatrix} \{\delta_{i-1}\} \\ \{\delta_i\} \end{Bmatrix} \quad (1)$$

where $\{F_i\}$ and $\{\delta_i\}$ are the vectors of the nodal forces and displacements at the i th node and $[K]$ is the element stiffness matrix. Consider a bar of constant cross-sectional area A subjected to a distributed axial load $p(x)$ and approximated by

finite elements where x denotes distance along the bar (fig. 1). For a bar finite element $\{F_i\}$ is the nodal extensional force, $\{\delta_i\}$ is the corresponding displacement u_i , and

$$[K] = \frac{EA}{h} \begin{bmatrix} 1 & -1 \\ -1 & 1 \end{bmatrix} \quad (2)$$

where h is the length of the element and E is Young's modulus.

In finite element methods distributed loads are replaced by concentrated loads at the node points. There are several possible ways in which distributed loads may be converted to concentrated loads. In this paper a very simple lumping procedure for loads is used for all finite element models. This procedure for the bar gives the concentrated load as the value of the distributed load at a grid point multiplied by one-half of the total length of the two adjoining elements. Treating the distributed load in this manner and utilizing equations (1) and (2) leads to the following equation for equilibrium at an i th point located between two segments of length h and αh (fig. 1)

$$\frac{EA}{h}(-u_{i-1} + u_i) + \frac{EA}{\alpha h}(u_i - u_{i+1}) = \frac{p_i h(1 + \alpha)}{2} \quad (3)$$

Equation (3) is a typical finite element equilibrium equation for the indicated approximation.

The behavior of the system of equation (3) is investigated as the number of equations approaches infinity and the size of the element vanishes. This is done by assuming the displacements u_i to be analytical functions and by examining equation (3) in the limit as h approaches zero with the aid of Taylor series expansion of displacements at points $i - 1$ and $i + 1$ about the i th point. This procedure results in

$$u'' - \frac{h}{3}(1 - \alpha)u'''' + \frac{h^2}{12}\left(\frac{1 + \alpha^3}{1 + \alpha}\right)u^{iv} + \dots + \frac{p}{EA} = 0 \quad (4)$$

where the primes denote differentiation with respect to x and where the subscript i has been omitted from u_i . (Omission of such subscripts is done consistently throughout this paper.) Equation (4) is the differential equation equivalent to the finite element equation at the i th node. This is a differential equation of infinite order and a detailed discussion of the solution of such equations is given in reference 6. The treatment of this equation herein is somewhat heuristic but satisfactory for the present results. The terms in equation (4) which are not multiplied by powers of h comprise exactly the governing differential equation for the continuous bar and the remaining terms are the discretization error in the differential equation that result from use of the finite element approximations. Thus equation (3) reduces to the correct continuum equation as h

approaches zero. The principal error in the differential equation resulting from the finite element approximation is the set of terms in the discretization error containing the lowest power of h . The power of h in the principal error denotes the order of the discretization error of the finite element equation and the rate of convergence as h vanishes. Thus the finite element equation leading to equation (4) has a discretization error of order h . Note that if the segments are equal ($\alpha = 1$), the discretization error is of order h^2 . Similarly, if the finite element equations do not converge to the governing differential equations, the discretization error would be of order h^0 or 1.

Harmonic Loading and Vibration Example

The error analysis procedure described in the previous section gives only the rate of convergence of the finite element approximation. The magnitude of the discretization error in the bar finite element approximation is now evaluated for the special case of a bar supported at each end, subjected to a sinusoidally distributed static loading

$$p = p_0 \sin \frac{m\pi x}{L} \quad (5)$$

and approximated by equal length elements. In equation (5) p_0 is the amplitude of the loading, m is the number of half waves, and L is the length of the bar. For this case equation (4) becomes

$$u'' + \frac{h^2}{12} u^{iv} + \dots + \frac{p_0}{EA} \sin \frac{m\pi x}{L} = 0 \quad (6)$$

A solution to this equation provides explicitly the error in the finite element approximation as a function of element size and harmonic wave length. If the loading is regarded as a continuous function, as was done in references 4 and 5, the exact solution to equation (6) is

$$u = u_0 \sin \frac{m\pi x}{L} \quad (7)$$

where u_0 is the amplitude of the displacement. Substitution of equation (7) into equation (6) results in

$$u = \frac{u_{ex}}{1 - \epsilon} \approx u_{ex}(1 + \epsilon) \quad (8)$$

where the exact solution to the bar for the sine loading is

$$u_{ex} = \frac{p_0}{EA} \left(\frac{L}{m\pi}\right)^2 \sin \frac{m\pi x}{L} \quad (9)$$

the principal error in deflection due to the finite element approximation is

$$\epsilon = \frac{\pi^2}{12N^2} \quad (10)$$

and the number of elements per harmonic half wave used to approximate the bar is

$$N = \frac{L/m}{h} \quad (11)$$

Error results for various values of N are as follows:

N	ϵ , percent
3	10
4	5
9	1

Thus approximately three elements per deflection half wave are needed to keep the error in finite element deflection calculations at a node to within 10 percent and nine elements per half wave to limit the error to 1 percent.

A similar approach is used to determine the error in natural frequency of the bar example when approximated by equal length elements. For vibration behavior where a simple lumping process analogous to that used for the distributed loading is used to obtain a diagonal mass matrix, the counterpart of equation (6) is

$$u'' + \frac{h^2}{12} u^{iv} + \dots + \frac{\bar{m}\omega^2}{EA} u = 0 \quad (12)$$

where \bar{m} is the mass per unit length and ω is the circular frequency. The vibration mode shape is the same as equation (7) and the eigenvalues of equation (12) are

$$\omega^2 = \omega_{ex}^2 (1 - \epsilon) \quad (13)$$

where

$$\omega_{ex}^2 = \left(\frac{L}{m\pi}\right)^2 \frac{EA}{m} \quad (14)$$

and ϵ is the discretization error due to the finite element approximation given by equation (10). Note that the error in the square of frequency is the same as that resulting from static deflection calculations except of opposite sign. Thus the frequency calculations converge from below and the deflection calculations converge from above.

For completeness, table I summarizes the principal error terms for the general bar finite element approximations and table II summarizes the evaluation of these errors for the harmonic response examples.

RESULTS AND DISCUSSION

The method described in the previous section was used to investigate the convergence of beam elements, straight and curved element approximations to an arch, rectangular and triangular plane stress elements, and plate bending elements. The results of the investigation are summarized in this section together with a general discussion. A summary of results of the error studies is given in tables I and II.

One-Dimensional Bending Element

For beam bending problems the well-known finite element model is based on the nodal variables

$$\{\delta_i\} = \begin{Bmatrix} w_i \\ \theta_i \end{Bmatrix} \quad (15)$$

where w_i is the displacement and θ_i the rotation at the i th node. (See fig. 2.) The governing differential equation for a beam is

$$w^{iv} = \frac{q}{EI} \quad (16)$$

where q is the lateral load, I is the moment of inertia of the beam cross section, and the constraint relationship between rotation and displacement is

$$\theta - w' = 0 \quad (17)$$

A satisfactory finite element approximation should converge to equations (16) and (17). As shown in appendix A (see also table I(a)), the beam element does converge with a principal error term of order h^4 .

The principal error was evaluated for a finite element approximation to a simply supported beam of length L subjected to sinusoidally distributed lateral load q where

$$q = q_0 \sin \frac{m\pi x}{L} \quad (18)$$

and where q_0 is a constant. The principal error in the lateral deflection w of the beam resulting from the finite element approximation is (see table II)

$$\epsilon = \frac{\pi^4}{720N^4} \quad (19)$$

Equation (19) also gives the magnitude of the error in frequency determination resulting from the finite element approximation. (See table II.)

Approximation of Curved Structures

Straight elements are often used to approximate curved structures such as curved beams, arches, and shells. To gain some insight into the influence of curvature, an arch of radius R was approximated by conventional straight beam elements which also had extensional capability. The arch loading is a normal pressure q and a tangential distributed loading p . (See fig. 3.) At a typical i th node three variables are required to define element behavior. For this problem it is convenient to take these variables as

$$\{\delta_i\} = \begin{Bmatrix} u_i \\ w_i \\ \theta_i \end{Bmatrix} \quad (20)$$

where u and w are the tangential and radial displacements, respectively, and θ is the rotation. Three finite element equations result from force and moment equilibrium. As the element size vanishes, the moment equilibrium equation at the i th node converges to the correct constraint equation between the rotation θ , radial displacement w , and tangential displacement u

$$\theta - \left(w' + \frac{u}{R} \right) = 0 \quad (21)$$

and the tangential and normal equilibrium equations converge, respectively, to

$$EA \left(-u'' + \frac{w'}{R} \right) - \frac{EI}{R} \left(w'''' + \frac{u''}{R} \right) - p = 0 \quad (22)$$

$$EI \left(w^{iv} + \frac{u''''}{R} \right) + EA \left(\frac{-u'}{R} + \frac{w}{R^2} \right) - q = 0 \quad (23)$$

where the principal error terms for equations (21) to (23) are proportional to h^2 . In equations (22) and (23) the rotation θ has been eliminated by using equation (21) in a manner similar to that done previously for the other bending problems. Equations (22) and (23) result when the cylindrical shell equations given in reference 7 are specialized to the case of an arch. Thus, the straight elements provide a convergent approximation to a first approximation arch theory with an error of order h^2 .

A study was also made of the use of curved elements to approximate a curved structure. The stiffness matrix for a curved element was derived based on the strain energy for a ring given in reference 8 and the details are given in appendix B. The displacements were approximated by assuming that arch tangential and normal displacements were linear and cubic, respectively, over the curved element length. The resulting finite element equations were investigated and the element pattern was found to converge to equation (21) plus the following equations with errors of order h^2 (see table I(a))

$$EA \left(-u'' + \frac{w'}{R} \right) - p = 0 \quad (24)$$

$$EI \left(w^{iv} + 2 \frac{w''}{R^2} + \frac{w}{R^4} \right) + EA \left(-\frac{u'}{R} + \frac{w}{R^2} \right) - q = 0 \quad (25)$$

The arch equations (24) and (25) are consistent with the ring strain energy given in reference 8 and are also the ring equations which result from the specialization of the cylindrical shell theory given in reference 9. Thus the curved elements also provide a convergent approximation to the curved structure with an error of order h^2 . The two sets of arch equations (22), (23) and (24), (25) are related in that the curvature terms differ by terms composed of the extensional strain divided by the arch radius. According to the Koiter criterion for thin shells (ref. 10) such modifications are admissible alternatives for a first approximation theory of shells, and it seems appropriate to use this criterion for arches.

An assessment of the magnitude of the discretization error terms for the straight and curved element approximations can be obtained by considering a closed circular ring subjected to a harmonic lateral loading and approximated by either straight or curved elements. For this problem

$$p = 0 \quad (26)$$

$$q = q_0 \sin \frac{mx}{R} \quad (27)$$

If the exact solutions to equations (22), (23) and (24), (25) are denoted as $\bar{u}_{ex}, \bar{w}_{ex}$ and u_{ex}, w_{ex} , respectively, these two solutions are related by

$$\bar{u}_{ex} = u_{ex} \left[1 + m^2 \left(\frac{\rho}{R} \right)^2 \right] \quad (28)$$

$$\bar{w}_{ex} = w_{ex} \left[1 + \left(\frac{\rho}{R} \right)^2 \right] \quad (29)$$

where ρ is the radius of gyration of the arch.

Because the determination of the magnitude of the principal error terms of order h^2 is quite tedious, selected numerical calculations were first carried out for the ring problem to investigate the magnitude of the error term. Results were obtained for several values of m and ring geometries. The numerical results indicated, as expected, that the convergence rate is proportional to $1/N^2$. Typical results for an arch with area of 1 inch² (6.45 cm²), moment of inertia of 10 inch⁴ (416 cm⁴), radius of 100 inches (2.54 m), and $m = 2$, approximated by 24 straight elements per half wave,

were $\epsilon_{\bar{u}} = -0.001955$ and $\epsilon_{\bar{w}} = -0.000892$ (see table II) where $u = \bar{u}_{\text{ex}}(1 + \epsilon_{\bar{u}})$ and $w = \bar{w}_{\text{ex}}(1 + \epsilon_{\bar{w}})$.

Results for the same problem based on a curved element approximation (using the same number of elements) were $\epsilon_u = \epsilon_w = -0.136862$. Because the size of ϵ_u and ϵ_w are quite large for the number of elements used for this example, the principal error terms of order h^2 were determined for the curved element approximation. These error terms for $u = u_{\text{ex}}(1 + \epsilon_u)$ and $w = w_{\text{ex}}(1 + \epsilon_w)$ (see table II) are

$$\epsilon_u = \epsilon_w = - \frac{\pi^2}{12N^2 \left(\frac{\rho}{R}\right)^2 (m^2 - 1)^2} \quad (m > 1) \quad (30)$$

Equation (30) shows that the principal error due to the curved element approximation is inversely proportional to the ratio $(\rho/R)^2$, which for a real arch is small but finite. Although this particular curved element approximation converges to the correct result, it has significant error for calculations based on a moderate number of elements and is an undesirable one. Thus a curved element may be developed which converges to the right equation, but the error may still be substantially greater than for the straight element. The reason for the undesirable character of the error term in equation (30) and the accuracy of the curved element used herein may be due to the fact that the usual displacements u and w do not admit unstressed rigid body motion of the arch element. Reference 11 has shown with numerical examples that omission of the rigid body modes in the element behavior appears to affect significantly the accuracy of curved structure approximations.

Two-Dimensional Plane Stress Elements

The linear elastic plane stress equations for equilibrium in the x- and y-directions formulated in terms of displacements are, respectively

$$u_{,xx} + \frac{1-\mu}{2} u_{,yy} + \frac{1+\mu}{2} v_{,xy} + \frac{p_x}{B} = 0 \quad (31)$$

$$\frac{1+\mu}{2} u_{,xy} + \frac{1-\mu}{2} v_{,xx} + v_{,yy} + \frac{p_y}{B} = 0 \quad (32)$$

Here u and v are the displacements in the x- and y-directions, respectively, p_x and p_y are the distributed forces, respectively, μ is Poisson's ratio, $B = \frac{Et}{1-\mu^2}$ is the extensional stiffness, and t is the plate thickness. Subscripts following a comma denote

differentiation with respect to the indicated variable. A satisfactory finite element approximation should lead to equations which converge to equations (31) and (32) at a node as the element size vanishes.

Rectangular elements.- The error analysis procedure is extended to a general rectangular plane stress element in appendix C and subsequently specialized for two models the stiffness properties of which are documented in reference 12. For the linear stress model the stresses σ_x and σ_y in the x- and y-directions, respectively, are assumed to vary linearly while the shear stress τ_{xy} is constant (fig. 4). For the linear edge displacement model, the displacements along an edge of the element are assumed to vary linearly (fig. 4). The nodal variables used to define the stiffness matrices for these finite elements are

$$\{\delta_i\} = \begin{Bmatrix} u_i \\ v_i \end{Bmatrix} \quad (33)$$

and a typical finite element equation contains contributions from all elements contiguous to the node. The pattern arrangement composed of equal elements is also shown in figure 4. The distributed forces on the plane stress body were again concentrated in a simple fashion based on the value of the distributed force at each node location. The typical finite element equations were obtained and the error terms evaluated. An investigation of the convergence of the finite element equilibrium equation for both models showed them to converge to the plane stress equations (31) and (32) with a principal error of order h^2 . (See table I(b).)

The principal error was evaluated for the case where the two types of rectangular elements were used to approximate a square plate in plane stress subjected to a harmonic inplane loading, in the y-direction. The loading is

$$p_x = 0 \quad (34)$$

$$p_y = p_0 \sin \frac{m\pi x}{a} \sin \frac{n\pi y}{a} \quad (35)$$

and the plate is supported on the boundary such that the force resultant in the x-direction and the displacement v both vanish. For $\mu = 0.3$ and $m = n$, the errors ϵ_u and ϵ_v , in the displacements u and v , respectively (see table II), are as follows:

Linear stress model

$$\epsilon_u = \frac{1.85}{N^2} \quad (36)$$

$$\epsilon_v = \frac{2.40}{N^2} \quad (37)$$

Linear edge displacement model

$$\epsilon_u = \frac{1.15}{N^2} \quad (38)$$

$$\epsilon_v = \frac{1.97}{N^2} \quad (39)$$

where N is the number of elements per half wave length.

Triangular elements.- Results were also obtained for the use of the classical triangular plate element (ref. 13) to approximate plane stress problems. Arrangements or patterns A, B, and C were investigated for the convergence of three right triangular elements (see fig. 5 for patterns about point i,j). It was found that pattern A converges to the required plane stress equations (see eqs. (31) and (32)) and the principal error is of order h^2 . However the corresponding equations for pattern B are

$$u_{,xx} + \frac{1-\mu}{2} u_{,yy} + \frac{p_x}{B} = 0 \quad (40)$$

$$\frac{1-\mu}{2} v_{,xx} + v_{,yy} + \frac{p_y}{B} = 0 \quad (41)$$

and for pattern C are

$$u_{,xx} + \frac{1-\mu}{2} u_{,yy} + (1+\mu)v_{,xy} + \frac{p_x}{B} = 0 \quad (42)$$

$$(1+\mu)u_{,xy} + \frac{1-\mu}{2} v_{,xx} + v_{,yy} + \frac{p_y}{B} = 0 \quad (43)$$

The additional error terms for all patterns proportional to h^2 are given in table I(b).

Some points can be noted by comparing the convergence characteristics when $h \rightarrow 0$ of the pattern B and C equations with equations (31) and (32). First of all both patterns B and C lead to a discretization error of order 1. The fact that the pattern B equations do not contain cross-derivative terms suggests that convergence of shear behavior at the nodal point is poor. This poor convergence is not unexpected since there is no mechanism in the finite element equations for representing changes in shear at the nodal point because of the arrangement of the elements. However the pattern C equations overprescribe the cross-derivative term by a factor of 2. Note that the difficulty arises from the element arrangement rather than the element properties since the element used here fully represents all states of plane stress. These results indicate that convergence difficulties may arise for some triangular elements as a result of poor element arrangement even though the element is well formulated.

Since the difficulty with pattern B is due to its inability to represent the cross derivative at the node, better convergence properties would be expected if additional degrees of freedom were used to characterize the right triangular element behavior. Such added degrees of freedom might be the deflections at the midpoint of the various edges or the derivatives of displacements at nodes.

Fortunately, if patterns B and C are used in structural idealizations, they usually occur in pairs (see fig. 5) and the underprediction of the shear stiffness at one point is compensated to some extent by an overprediction of shear stiffness at a neighboring point. Nevertheless these results suggest that caution should be exercised to ensure that an excessive number of either patterns B or C does not occur in a structure when the results are strongly dependent on shear stiffness. A more consistent approach is to use pattern A since it converges to the appropriate plane stress equation.

For completeness the convergence of a pattern composed of equilateral triangles in plane stress was also investigated. The typical pattern is shown in figure 6 and the resulting finite element equations were found to converge to the plane stress equations with a principal error of order h^2 . (See table I(b).)

Two-Dimensional Plate Bending Elements

The error analysis procedure was developed for a general rectangular plate bending element in appendix D and subsequently specialized for three models. The models investigated were those developed by Papenfuss (ref. 14), Melosh (ref. 15), and one developed independently by Adini and Clough (see ref. 1 or ref. 16) and Melosh (ref. 17). (These will be denoted respectively as the Papenfuss, Melosh, and ACM models; the stiffness matrices of all three models are tabulated conveniently in ref. 1.) The pattern arrangement is shown in figure 7. The nodal variables for these finite element models are

$$\{\delta_i\} = \begin{Bmatrix} w_i \\ \theta_i \\ \varphi_i \end{Bmatrix} \quad (44)$$

where w is the lateral displacement and θ and φ are the rotations about the y - and x -axes, respectively. On the basis of the beam results a consistent set of three plate bending finite element equations should be expected to converge to

$$\nabla^4 w = \frac{q}{D} \quad (45)$$

$$\theta = w_{,x} \quad (46)$$

$$\varphi = w_{,y} \quad (47)$$

as the element size vanishes. Here equation (45) is the familiar plate equation and equations (46) and (47) are constraint equations between the rotations θ and φ and the derivative of w . All three models lead to equations which converge to constraint equations of the form of equations (46) and (47) and the Melosh and ACM models also converge to the plate equation (45). The Papenfuss model however converges to the equation

$$\nabla^4 w + \left(\frac{2\alpha^2}{35} + \frac{2}{35\alpha^2} + \frac{2}{25} \right) w_{,xxyy} = \frac{q}{D} \quad (48)$$

where α is the aspect ratio of the element and thus has a principal error of order 1. The principal errors for all other equations for the three models are proportional to h^2 with the exception of the constraint equations for the ACM model which are proportional to h^4 . (See table I(c).)

It is well known from numerical calculations (ref. 1) that the Papenfuss model has some deficiencies and that the source of the discrepancies is the inability of the model to describe the twist behavior of a plate. This discrepancy term shows up as an incorrect cross-derivative term in equation (48) when h vanishes.

Square elements of the three models were used to approximate a simply supported square plate subjected to a harmonic loading

$$q = q_0 \sin \frac{m\pi x}{a} \sin \frac{n\pi x}{a} \quad (49)$$

The same procedure was used to approximate the lateral vibration characteristics of the plate. The error in deflection ϵ_1 and the error in frequency ϵ_2 resulting from the finite element approximation for $m = n$ and $\mu = 0.3$ (see table II) are as follows:

Model	ϵ_1	ϵ_2
Papenfuss	$-0.0463 - \frac{0.2646}{N^2}$	$-0.0486 - \frac{0.2909}{N^2}$
Melosh	$\frac{0.708}{N^2}$	$\frac{0.708}{N^2}$
ACM	$\frac{1.069}{N^2}$	$\frac{1.069}{N^2}$

where $N = \frac{a/m}{h}$ is the number of elements per Fourier half wave. Figure 8 shows a sketch of the plate and a plot of the ratio of the finite element results to the exact result for the three elements as $1/N^2$ vanishes. The results show that in the limit as the size

of the element vanishes, the results for this problem based on the Papenfuss model have an error of approximately 5 percent. Note also that the Papenfuss model converges from below and the other two models converge from above.

Since the Papenfuss model equations do not converge to the plate equation, a solution was obtained for the resulting Papenfuss psuedoplate equation (48) for a rectangular planform subjected to a uniform pressure \bar{q} , having simple support boundary conditions and approximated by elements having the same aspect ratio as the plate. The solution was obtained by means of classical Fourier series expansions of the load \bar{q} and deflection shape as

$$\bar{q} = \sum_{m=1}^{\infty} \sum_{n=1}^{\infty} q_{mn} \sin \frac{m\pi x}{a} \sin \frac{n\pi y}{b} \quad (50)$$

$$w = \sum_{m=1}^{\infty} \sum_{n=1}^{\infty} w_{mn} \sin \frac{m\pi x}{a} \sin \frac{n\pi y}{b} \quad (51)$$

where a and b are the lengths of the plate in the x - and y -directions, respectively, and m and n are restricted to the odd integers.

The quantities w_{mn} are related to the pressure \bar{q} by

$$w_{mn} = \frac{16\bar{q}}{\pi^6 D_{mn} \left[\frac{m^4}{a^4} + \frac{m^2 n^2}{a^2 b^2} \left(\frac{52}{25} + \frac{2\alpha^2}{35} + \frac{2}{35\alpha^2} \right) + \frac{n^4}{b^4} \right]} \quad (52)$$

The following table compares the center deflection w_c of the Papenfuss psuedoplate with the exact plate results for $\frac{w_c D}{\bar{q} a^4} \times 10^3$:

a/b	Papenfuss psuedoplate	Exact plate
1	3.87	4.06
1/2	9.64	10.13

These results indicate that the Papenfuss psuedoplate has an error of approximately 5 percent for both cases. Numerical results obtained in reference 1 for these cases appear to be converging toward these analytical results.

Remarks on Finite Element and Finite Difference Approximations

Some general results can be deduced by comparing the convergence and principal error results of the various element approximations. One result deals with the requirement of interelement compatibility. Consideration of the elements for both plane stress and bending gave examples where this requirement was neither necessary nor sufficient to insure convergence. The rectangular linear stress model is not interelement compatible in displacements and the rectangular Melosh and ACM bending models are not compatible in slope; yet these three converge to the correct equations. On the other hand the right triangular plane stress patterns B and C are interelement compatible in displacements and the Papenfuss plate bending element is compatible in slope and displacements and yet these elements and arrangements do not converge to the correct equations.

Some influence of unequal length segments is seen from the change in principal errors for the bar approximations. For bar elements of equal length the principal error is proportional to h^2 , and for bars of unequal length, proportional to h . From the asymmetric character of the Taylor series expansion about the reference point similar reduction of the order of error would be expected for other elements. This slower rate of convergence suggests that results may be less accurate when structures are approximated by unequal elements than when approximated by equal length segments.

Comparison of the errors for the plane stress elements with those of the bar elements for the case of harmonic loading indicates that approximately nine bar elements and 15 square plane stress elements per half wave in one direction are required for a 1-percent error. Approximately two beam elements and nine square Melosh plate bending elements are required for a 1-percent error. Thus more elements are required per wavelength in one direction for two-dimensional behavior than for one-dimensional behavior to obtain the same degree of accuracy. This fact is important because practical complex structures such as stiffened plates or shells are two dimensional and usually are approximated by various combinations of one- and two-dimensional elements. Since the elements have varying degrees of accuracy, results obtained for a structure approximated by a combination of the elements may be biased in some sense rather than having uniform inaccuracies.

Results are given in appendix E which compares finite element approximations and central finite difference approximations to differential equations for the same problem. The results show that for bar, beam, and plane stress equations some correlation can be made between finite difference equations and equations resulting from finite element approximations. The results for the harmonic load problem for plane stress show that neither method is always more accurate and that the value of Poisson's ratio can change the relative accuracies of finite difference and finite element results. The results also show that the finite element approximations to beam problems are usually more accurate

than central finite difference approximations because of the higher rate of convergence of the finite element approximation.

CONCLUDING REMARKS

Basic data are presented on the convergence and accuracy of finite element equations resulting from patterns and elements in common use. The elements studied include bar elements, beam elements, plane stress elements of rectangular and triangular shape, plate bending elements of rectangular shape and straight and curved arch elements. The results indicate that many of the elements and patterns have good convergence properties; that is, the resulting finite element equations at a node converge to the continuum equations at the node as the element size vanishes. The results also indicate that some elements and/or patterns have poor convergence properties. Right triangular plane stress patterns, for example, can have undesirable convergence properties. It is shown that the requirement for interelement compatibility is neither necessary nor sufficient to guarantee convergence of the finite element equations. Results for arch approximations show that both straight elements and curved elements converge to the behavior of an arch structure; however for the problem considered, the straight element approximation gives substantially better results than the curved element derived herein.

Langley Research Center,
National Aeronautics and Space Administration,
Langley Station, Hampton, Va., December 16, 1969.

APPENDIX A

ONE-DIMENSIONAL BENDING ELEMENT

When bending behavior is introduced, finite element models and the discretization error analysis procedure become more complex than for extensional elements. To indicate the additional features brought on by bending, consider a simple prismatic beam subjected to distributed load q and approximated by an assemblage of beam bending finite elements of equal length h (fig. 2). The finite element nodal variables for this problem are

$$\{\delta_i\} = \begin{Bmatrix} w_i \\ \theta_i \end{Bmatrix} \quad (A1)$$

where w_i and θ_i are the displacement and rotation, respectively, at a node, and two finite element equilibrium equations are obtained at each node. These two equations are expanded in a Taylor series about the i th point (when w and θ are considered as independent variables) to give

$$\begin{aligned} -12w'' - h^2w^{iv} - \frac{h^4}{30}w^{vi} - \frac{h^6}{1680}w^{viii} + \dots + 12\theta' + 2h^2\theta''' + \frac{h^4}{10}\theta^v \\ + \frac{h^6}{420}\theta^{vii} + \dots = \frac{qh^2}{EI} \end{aligned} \quad (A2)$$

$$\theta = w' + \frac{h^2}{6}w''' + \frac{h^4}{120}w^v + \frac{h^6}{5040}w^{vii} + \dots - \frac{h^2}{6}\theta'' - \frac{h^4}{72}\theta^{iv} - \frac{h^6}{2160}\theta^{vi} + \dots \quad (A3)$$

where I is the moment of inertia of the beam cross section. Since beam behavior for a continuum is defined by only one independent variable w , it is useful to eliminate θ insofar as possible from the finite element equation. This elimination is done by differentiating equation (A3) to obtain expressions for derivatives of θ and sequentially back substituting these derivatives into both equations (A2) and (A3).

Equations (A2) and (A3) finally can be put in the form

$$w^{iv} - \frac{h^4}{720}w^{viii} + \dots = \frac{q}{EI} \quad (A4)$$

$$\theta - w' + \frac{h^4}{180}w^v + \dots = 0 \quad (A5)$$

Equations (A4) and (A5) show that in the limit as h vanishes the beam finite element equations converge to the familiar beam equation and the correct constraint equation between the two finite element variables θ and w .

APPENDIX B

DERIVATION OF STIFFNESS MATRIX OF A CURVED BEAM

In this section the stiffness matrix of a curved prismatic beam bending and extensional element is derived. The method used is the Rayleigh-Ritz method wherein the strain energy for the element is expressed in the matrix form

$$U = \frac{1}{2} \{\delta\}^T [K] \{\delta\} \quad (B1)$$

where $\{\delta\}$ is the set of generalized displacements that characterize the element and $[K]$ is the stiffness matrix. The energy for a curved beam of radius R and length h based on the theory of reference 8 is

$$U = \frac{1}{2} \int_0^h \int_A \{b\}^T [C] \{b\} dA ds \quad (B2)$$

where

$$\{b\} = \begin{Bmatrix} u' \\ w \\ \theta' \end{Bmatrix} \quad (B3)$$

$$[C] = \frac{E}{R(R - \zeta)} \begin{bmatrix} R^2 & -R & -R^2\zeta \\ -R & 1 & R\zeta \\ -R^2\zeta & R\zeta & R^2\zeta^2 \end{bmatrix} \quad (B4)$$

and

$$\theta = w' + \frac{u}{R} \quad (B5)$$

In the preceding equations u and w are, respectively, the tangential and radial displacement of the element, and s and ζ are, respectively, the coordinates along the length and through the depth of the element.

The displacements are assumed to vary over the element length as

$$w = a_0 + a_1 s + a_2 s^2 + a_3 s^3 \quad (B6)$$

$$u = b_0 + b_1 s \quad (B7)$$

APPENDIX B – Continued

where a_k and b_k are constants. The nodal variables may then be related to the constants as

$$\{\delta\} = [H]\{a\} \quad (B8)$$

where

$$[H] = \begin{bmatrix} 0 & 0 & 0 & 0 & 1 & 0 \\ 1 & 0 & 0 & 0 & 0 & 0 \\ 0 & 1 & 0 & 0 & \frac{1}{R} & 0 \\ 0 & 0 & 0 & 0 & 1 & h \\ 1 & h & h^2 & h^3 & 0 & 0 \\ 0 & 1 & 2h & 3h^2 & \frac{1}{R} & \frac{h}{R} \end{bmatrix} \quad (B9)$$

$$\{\delta\} = \begin{Bmatrix} u_1 \\ w_1 \\ \theta_1 \\ u_2 \\ w_2 \\ \theta_2 \end{Bmatrix} \quad (B10)$$

$$\{a\} = \begin{Bmatrix} a_0 \\ a_1 \\ a_2 \\ a_3 \\ b_0 \\ b_1 \end{Bmatrix} \quad (B11)$$

and the subscript 1 in the $\{\delta\}$ vector indicates the end of the element where $s = 0$, and the subscript 2 in the vector indicates the end of the element where $s = h$. Differentiation and substitution of equations (B6) and (B7) into equation (B3) yields

$$\{b\} = [B]\{a\} \quad (B12)$$

APPENDIX B - Continued

where

$$[B] = \begin{bmatrix} 0 & 0 & 0 & 0 & 0 & 1 \\ 1 & s & s^2 & s^3 & 0 & 0 \\ 0 & 0 & 2 & 6s & 0 & \frac{1}{R} \end{bmatrix} \quad (B13)$$

Equation (B2) through the use of equations (B12) and (B8) may be rewritten as

$$U = \frac{1}{2} \int_0^h \int_A \{\delta\}^T [H^{-1}]^T [B]^T [C] [B] [H^{-1}] \{\delta\} dA ds \quad (B14)$$

Since $[H]$ and $[B]$ are independent of the integration over the cross section, the energy may be expressed as

$$U = \frac{1}{2} \int_0^h \{\delta\}^T [H^{-1}]^T [B]^T [T] [B] [H^{-1}] \{\delta\} ds \quad (B15)$$

where

$$[T] = \int_A [C] dA = \frac{EA}{R} \begin{bmatrix} R(1+Z) & -(1+Z) & -R^2Z \\ -(1+Z) & \frac{1}{R}(1+Z) & RZ \\ -R^2Z & RZ & R^3Z \end{bmatrix} \quad (B16)$$

The following integrals were used to obtain equations (B16)

$$\left. \begin{aligned} \int \frac{dA}{R-\xi} &= \frac{A}{R}(1+Z) \\ \int \frac{\xi dA}{R-\xi} &= ZA \\ \int \frac{\xi^2 dA}{R-\xi} &= ZAR \end{aligned} \right\} \quad (B17)$$

where Z is the Winkler-Bach constant for curved beams. Thus a comparison of equations (B1) and (B15) reveals that

$$[K] = \int_0^h [H^{-1}]^T [B]^T [T] [B] [H^{-1}] ds \quad (B18)$$

APPENDIX B – Continued

The elements of the stiffness matrix are

$$\begin{aligned}
 [K] = & \begin{bmatrix} k_{11} & k_{12} & k_{13} & k_{14} & k_{15} & k_{16} \\ & k_{22} & k_{23} & k_{24} & k_{25} & k_{26} \\ & & k_{33} & k_{34} & k_{35} & k_{36} \\ & \text{Symmetric} & & k_{44} & k_{45} & k_{46} \\ & & & & k_{55} & k_{56} \\ & & & & & k_{66} \end{bmatrix} \qquad (B19)
 \end{aligned}$$

where

$$\begin{aligned}
 k_{11} &= \frac{EA}{R} \left[\frac{1}{\beta} - \frac{\beta}{6} + \frac{\beta^3}{105} + Z \left(\frac{4}{\beta} - \frac{4\beta}{15} + \frac{\beta^3}{105} \right) \right] \\
 k_{12} &= \frac{EA}{R} \left[\frac{1}{2} - \frac{11\beta^2}{210} + Z \left(\frac{6}{5} - \frac{6}{\beta^2} - \frac{11\beta^2}{210} \right) \right] \\
 k_{22} &= \frac{EA}{R} \left[\frac{13\beta}{35} + Z \left(\frac{13\beta}{35} - \frac{12}{5\beta} + \frac{12}{\beta^3} \right) \right] \\
 k_{13} &= EA \left[\frac{\beta}{12} - \frac{\beta^3}{105} + Z \left(\frac{4\beta}{15} - \frac{\beta^3}{105} - \frac{4}{\beta} \right) \right] \\
 k_{23} &= EA\beta \left[\frac{11\beta}{210} + Z \left(\frac{11\beta}{210} - \frac{6}{5\beta} + \frac{6}{\beta^3} \right) \right] \\
 k_{33} &= EAR\beta \left[\frac{\beta^2}{105} + Z \left(-\frac{4}{15} + \frac{\beta^2}{105} + \frac{4}{\beta^2} \right) \right] \\
 k_{14} &= \frac{EA}{R} \left[\frac{\beta}{6} - \frac{1}{\beta} - \frac{\beta^3}{140} + Z \left(\frac{\beta}{15} + \frac{2}{\beta} - \frac{\beta^3}{140} \right) \right] \\
 k_{24} &= \frac{EA}{R} \left[-\frac{1}{2} + \frac{13\beta^2}{420} + Z \left(\frac{1}{5} + \frac{13\beta^2}{420} - \frac{6}{\beta^2} \right) \right] \\
 k_{34} &= EA\beta \left[-\frac{1}{12} + \frac{\beta^2}{140} + Z \left(-\frac{1}{15} + \frac{\beta^2}{140} - \frac{2}{\beta^2} \right) \right]
 \end{aligned}$$

(Equation continued on next page)

APPENDIX B - Concluded

$$\begin{aligned}
 k_{44} &= \frac{EA}{R} \left[-\frac{\beta}{6} + \frac{1}{\beta} + \frac{\beta^3}{105} + Z \left(-\frac{4\beta}{15} + \frac{4}{\beta} + \frac{\beta^3}{105} \right) \right] \\
 k_{15} &= \frac{EA}{R} \left[\frac{1}{2} - \frac{13\beta^2}{420} + Z \left(-\frac{1}{5} - \frac{13\beta^2}{420} + \frac{6}{\beta^2} \right) \right] \\
 k_{25} &= \frac{EA}{R} \left[\frac{9\beta}{70} + Z \left(\frac{9\beta}{70} + \frac{12}{5\beta} - \frac{12}{\beta^3} \right) \right] \\
 k_{35} &= EA\beta \left[\frac{13\beta}{420} + Z \left(\frac{13\beta}{420} + \frac{1}{5\beta} - \frac{6}{\beta^3} \right) \right] \\
 k_{45} &= \frac{EA}{R} \left[-\frac{1}{2} + \frac{11\beta^2}{210} + Z \left(-\frac{6}{5} + \frac{11\beta^2}{210} + \frac{6}{\beta^2} \right) \right] \\
 k_{55} &= \frac{EA}{R} \left[\frac{13\beta}{35} + Z \left(\frac{13\beta}{35} - \frac{12}{5\beta} + \frac{12}{\beta^3} \right) \right] \\
 k_{16} &= EA\beta \left[-\frac{1}{12} + \frac{\beta^2}{140} + Z \left(-\frac{1}{15} + \frac{\beta^2}{140} - \frac{2}{\beta^2} \right) \right] \\
 k_{26} &= EA\beta \left[-\frac{13\beta}{420} + Z \left(-\frac{13\beta}{420} - \frac{1}{5\beta} + \frac{6}{\beta^3} \right) \right] \\
 k_{36} &= EAR\beta^2 \left[-\frac{\beta}{140} + Z \left(-\frac{\beta}{140} + \frac{1}{15\beta} + \frac{2}{\beta^3} \right) \right] \\
 k_{46} &= EA\beta \left[\frac{1}{12} - \frac{\beta^2}{105} + Z \left(\frac{4}{15} - \frac{\beta^2}{105} - \frac{4}{\beta^2} \right) \right] \\
 k_{56} &= EA\beta \left[-\frac{11\beta}{210} + Z \left(-\frac{11\beta}{210} + \frac{6}{5\beta} - \frac{6}{\beta^3} \right) \right] \\
 k_{66} &= EAR\beta \left[\frac{\beta^2}{105} + Z \left(-\frac{4}{15} + \frac{\beta^2}{105} + \frac{4}{\beta^2} \right) \right]
 \end{aligned} \tag{B20}$$

where

$$\beta = \frac{h}{R} \tag{B21}$$

In the error analysis study in the body of the paper, it is assumed that $\zeta \ll R$. Then Z may be approximated by

$$Z = \frac{1}{AR^2} \tag{B22}$$

APPENDIX C

RECTANGULAR PLANE STRESS ELEMENTS

This appendix presents the development of accuracy relationships for plane stress problems approximated by finite elements. Consider an isotropic constant thickness body in plane stress subjected to distributed inplane loadings p_x and p_y and approximated by rectangular finite elements (fig. 4). It is presumed that the only generalized coordinates used to describe the element behavior are the displacements u and v at the nodes. The rectangular plane stress finite elements are connected at the corners; however the displacements of two adjacent elements need not match along a common boundary; that is, the elements need not be interelement compatible.

The behavior of a body in plane stress is governed by two equations of equilibrium. In typical finite element approximations, two equilibrium equations also occur at each node if the stiffness matrix of a typical rectangular finite element has the general form

$$\begin{Bmatrix} F_{x1} \\ F_{y1} \\ F_{x2} \\ F_{y2} \\ F_{x3} \\ F_{y3} \\ F_{x4} \\ F_{y4} \end{Bmatrix} = \begin{bmatrix} k_{11} & k_{12} & k_{13} & k_{14} & k_{15} & k_{16} & k_{17} & k_{18} \\ & k_{22} & k_{23} & k_{24} & k_{25} & k_{26} & k_{27} & k_{28} \\ & & k_{33} & k_{34} & k_{35} & k_{36} & k_{37} & k_{38} \\ & & & k_{44} & k_{45} & k_{46} & k_{47} & k_{48} \\ & & & & k_{55} & k_{56} & k_{57} & k_{58} \\ & \text{Symmetric} & & & & k_{66} & k_{67} & k_{68} \\ & & & & & & k_{77} & k_{78} \\ & & & & & & & k_{88} \end{bmatrix} \begin{Bmatrix} u_1 \\ v_1 \\ u_2 \\ v_2 \\ u_3 \\ v_3 \\ u_4 \\ v_4 \end{Bmatrix} \quad (C1)$$

where u_i and v_i are the displacements of the i th node in the x - and y -directions, respectively, and F_{x_i} and F_{y_i} are the corresponding element nodal forces (fig. 4), and the quantities k_{ij} are the stiffness matrix coefficients which depend on the behavior assumed within the element. The nodal concentrated load is taken to be the pressure evaluated at that grid point multiplied by $1/4$ of the total area of the four elements surrounding the grid point. Use of equation (C1) for each of four adjacent identical elements leads to the following two finite element equations at a node i, j

APPENDIX C – Concluded

$$\begin{aligned}
 &4k_{11}u_{i,j} + 2k_{13}(u_{i+1,j} + u_{i-1,j}) + k_{15}(u_{i+1,j+1} + u_{i-1,j+1} + u_{i-1,j-1} + u_{i+1,j-1}) \\
 &+ 2k_{17}(u_{i,j+1} + u_{i,j-1}) + k_{16}(v_{i+1,j+1} - v_{i-1,j+1} + v_{i-1,j-1} - v_{i+1,j-1}) - p_x \alpha h^2 = 0 \quad (C2)
 \end{aligned}$$

$$\begin{aligned}
 &k_{25}(u_{i+1,j+1} - u_{i-1,j+1} + u_{i-1,j-1} - u_{i+1,j-1}) + 4k_{22}v_{i,j} + 2k_{24}(v_{i+1,j} + v_{i-1,j}) \\
 &+ k_{26}(v_{i+1,j+1} + v_{i-1,j+1} + v_{i-1,j-1} + v_{i+1,j-1}) + 2k_{28}(v_{i,j+1} + v_{i,j-1}) - p_y \alpha h^2 = 0 \quad (C3)
 \end{aligned}$$

The variables u and v in equations (C2) and (C3) are expanded in a two-dimensional Taylor series about the point i,j to give

$$\begin{aligned}
 &4(k_{11} + k_{13} + k_{15} + k_{17})u + 2h^2 \left[(k_{13} + k_{15})u_{,xx} + \alpha^2(k_{15} + k_{17})u_{,yy} + 2\alpha k_{16}v_{,xy} \right] \\
 &+ \frac{h^4}{6} \left[(k_{13} + k_{15})u_{,xxxx} + 6\alpha^2 k_{15}u_{,xxyy} + \alpha^4(k_{15} + k_{17})u_{,yyyy} + 4k_{16}(\alpha v_{,xxyy} + \alpha^3 v_{,xyyy}) \right] \\
 &+ \dots - p_x \alpha h^2 = 0 \quad (C4)
 \end{aligned}$$

$$\begin{aligned}
 &4(k_{22} + k_{24} + k_{26} + k_{28})v + 2h^2 \left[(k_{24} + k_{26})v_{,xx} + \alpha^2(k_{26} + k_{28})v_{,yy} + 2\alpha k_{25}u_{,xy} \right] \\
 &+ \frac{h^4}{6} \left[(k_{24} + k_{26})v_{,xxxx} + 6\alpha^2 k_{26}v_{,xxyy} + \alpha^4(k_{26} + k_{28})v_{,yyyy} + 4k_{25}(\alpha u_{,xxyy} + \alpha^3 u_{,xyyy}) \right] \\
 &+ \dots - p_y \alpha h^2 = 0 \quad (C5)
 \end{aligned}$$

where the subscripts following a comma denote differentiation with respect to the indicated variable. Equations (C4) and (C5), which represent equilibrium in x - and y -directions, respectively, can be used to investigate the convergence characteristics of any plane stress rectangular element with a stiffness matrix of the form of equation (C1).

APPENDIX D

RECTANGULAR PLATE BENDING ELEMENTS

The development of finite element models for plate bending problems is less obvious than for beams, and several plate bending models, each derived from different assumptions, are in current use. Many of the models have three independent variables at each grid point; namely, the displacement w , the rotation θ about the y -axis, and the rotation φ about the x -axis. (See fig. 7.) This section describes the error analysis procedure for a rectangular isotropic constant-thickness plate bending element the behavior of which is described by these three nodal variables. For a rectangular model of length h in the x -direction and width αh in the y -direction, the stiffness matrix can be put in the form

$$\left\{ \begin{array}{l} F_1 \\ \left(\frac{M_x}{h}\right)_1 \\ \left(\frac{M_y}{\alpha h}\right)_1 \\ F_2 \\ \left(\frac{M_x}{h}\right)_2 \\ \left(\frac{M_y}{\alpha h}\right)_2 \\ F_3 \\ \left(\frac{M_x}{h}\right)_3 \\ \left(\frac{M_y}{\alpha h}\right)_3 \\ F_4 \\ \left(\frac{M_x}{h}\right)_4 \\ \left(\frac{M_y}{\alpha h}\right)_4 \end{array} \right\} = \frac{D}{\alpha h^2} \left[\begin{array}{cccccccccccc} k_{11} & k_{12} & k_{13} & k_{14} & k_{15} & k_{16} & k_{17} & k_{18} & k_{19} & k_{1,10} & k_{1,11} & k_{1,12} \\ & k_{22} & k_{23} & k_{24} & k_{25} & k_{26} & k_{27} & k_{28} & k_{29} & k_{2,10} & k_{2,11} & k_{2,12} \\ & & k_{33} & k_{34} & k_{35} & k_{36} & k_{37} & k_{38} & k_{39} & k_{3,10} & k_{3,11} & k_{3,12} \\ & & & k_{44} & k_{45} & k_{46} & k_{47} & k_{48} & k_{49} & k_{4,10} & k_{4,11} & k_{4,12} \\ & & & & k_{55} & k_{56} & k_{57} & k_{58} & k_{59} & k_{5,10} & k_{5,11} & k_{5,12} \\ & & & & & k_{66} & k_{67} & k_{68} & k_{69} & k_{6,10} & k_{6,11} & k_{6,12} \\ & & & & & & k_{77} & k_{78} & k_{79} & k_{7,10} & k_{7,11} & k_{7,12} \\ & & & & & & & k_{88} & k_{89} & k_{8,10} & k_{8,11} & k_{8,12} \\ & & & & & & & & k_{99} & k_{9,10} & k_{9,11} & k_{9,12} \\ & & & & & & & & & k_{10,11} & k_{10,11} & k_{10,10} \\ & & & & & & & & & & k_{11,11} & k_{11,12} \\ & & & & & & & & & & & k_{12,12} \end{array} \right] \left\{ \begin{array}{l} w_1 \\ h\theta_1 \\ \alpha h\varphi_1 \\ w_2 \\ h\theta_2 \\ \alpha h\varphi_2 \\ w_3 \\ h\theta_3 \\ \alpha h\varphi_3 \\ w_4 \\ h\theta_4 \\ \alpha h\varphi_4 \end{array} \right\} \quad (D1)$$

APPENDIX D - Continued

where the quantities k_{ij} are the stiffness matrix coefficients which depend on the behavior assumed within the element and where the directions of rotations and moments are defined in figure 7. Let a continuous plate subjected to a lateral load q be represented by an assemblage of rectangular finite elements the stiffness properties of which are given in the form of equation (D1). The three finite equations at a node i,j are

$$\begin{aligned} & \frac{D}{\alpha h^2} \left[4k_{11}w_{i,j} + 2k_{14}(w_{i+1,j} + w_{i-1,j}) + 2k_{17}(w_{i,j+1} + w_{i,j-1}) + k_{1,10}(w_{i+1,j+1} + w_{i-1,j+1} \right. \\ & + w_{i-1,j-1} + w_{i+1,j-1}) + 2hk_{15}(\theta_{i+1,j} - \theta_{i-1,j}) + hk_{1,11}(\theta_{i+1,j+1} - \theta_{i-1,j+1} - \theta_{i-1,j-1} \\ & + \theta_{i+1,j-1}) + 2\alpha hk_{19}(\varphi_{i,j+1} - \varphi_{i,j-1}) + \alpha hk_{1,12}(\varphi_{i+1,j+1} + \varphi_{i-1,j+1} - \varphi_{i-1,j-1} \\ & \left. - \varphi_{i+1,j-1}) \right] = q\alpha h^2 \end{aligned} \quad (D2)$$

$$\begin{aligned} & \frac{D}{\alpha h^2} \left[4hk_{22}\theta_{i,j} + 2hk_{25}(\theta_{i+1,j} + \theta_{i-1,j}) + 2hk_{28}(\theta_{i,j+1} + \theta_{i,j-1}) + hk_{2,11}(\theta_{i+1,j+1} + \theta_{i-1,j+1} \right. \\ & + \theta_{i-1,j-1} + \theta_{i+1,j-1}) + 2k_{24}(w_{i+1,j} - w_{i-1,j}) + k_{2,10}(w_{i+1,j+1} - w_{i-1,j+1} - w_{i-1,j-1} \\ & \left. + w_{i+1,j-1}) + \alpha hk_{2,12}(\varphi_{i+1,j+1} - \varphi_{i-1,j+1} + \varphi_{i-1,j-1} - \varphi_{i+1,j-1}) \right] = 0 \end{aligned} \quad (D3)$$

$$\begin{aligned} & \frac{D}{\alpha h^2} \left[4\alpha hk_{33}\varphi_{i,j} + 2\alpha hk_{36}(\varphi_{i+1,j} + \varphi_{i-1,j}) + 2\alpha hk_{39}(\varphi_{i,j+1} + \varphi_{i,j-1}) + \alpha hk_{3,12}(\varphi_{i+1,j+1} \right. \\ & + \varphi_{i-1,j+1} + \varphi_{i-1,j-1} + \varphi_{i+1,j-1}) + 2k_{37}(w_{i,j+1} - w_{i,j-1}) + k_{3,10}(w_{i+1,j+1} + w_{i-1,j+1} \\ & \left. - w_{i-1,j-1} - w_{i+1,j-1}) + hk_{3,11}(\theta_{i+1,j+1} - \theta_{i-1,j+1} + \theta_{i-1,j-1} - \theta_{i+1,j-1}) \right] = 0 \end{aligned} \quad (D4)$$

where D is the bending stiffness of the plate.

The quantities w , θ , and φ in equations (D3) and (D4) are expanded in the Taylor series about the point i,j and through a process of differentiation and back substitution the quantities θ and φ are expressed in terms of w . The result is

APPENDIX D - Continued

$$\theta = -\frac{k_{24} + k_{2,10}}{K_1} w_{,x} - \frac{h^2}{2K_1} \left\{ (k_{24} + k_{2,10}) \left(\frac{1}{3} - \frac{k_{25} + k_{2,11}}{K_1} \right) w_{,xxx} \right. \\ \left. + \alpha^2 \left[k_{2,10} - \frac{k_{24} + k_{2,10}}{K_1} (k_{28} + k_{2,11}) - 2k_{2,12} \frac{k_{37} + k_{3,10}}{K_2} \right] w_{,xyy} \right\} + O(h^4) \quad (D5)$$

$$\varphi = -\frac{k_{37} + k_{3,10}}{K_2} w_{,y} - \frac{h^2}{2K_2} \left\{ \left[k_{3,10} - (k_{36} + k_{3,12}) \frac{k_{37} + k_{3,10}}{K_2} \right. \right. \\ \left. \left. - 2k_{3,11} \frac{k_{24} + k_{2,10}}{K_1} \right] w_{,xxy} + \alpha^2 (k_{37} + k_{3,10}) \left(\frac{1}{3} - \frac{k_{39} + k_{3,12}}{K_2} \right) w_{,yyy} \right\} + O(h^4) \quad (D6)$$

where

$$\left. \begin{aligned} K_1 &= k_{22} + k_{25} + k_{28} + k_{2,11} \\ K_2 &= k_{33} + k_{36} + k_{39} + k_{3,12} \end{aligned} \right\} \quad (D7)$$

Equation (D2) is similarly expanded in Taylor series and equations (D5) and (D6) are used to eliminate θ and φ . The result is

$$4(k_{11} + k_{14} + k_{17} + k_{1,10})w + h^2 \left[2(k_{14} + k_{1,10}) - 4(k_{15} + k_{1,11}) \frac{k_{24} + k_{2,10}}{K_1} \right] w_{,xx} \\ + \alpha^2 h^2 \left[2(k_{17} + k_{1,10}) - 4(k_{19} + k_{1,12}) \frac{k_{37} + k_{3,10}}{K_2} \right] w_{,yy} + h^4 \left[\frac{1}{6}(k_{14} + k_{1,10}) \right. \\ \left. - (k_{15} + k_{1,11}) \left(\frac{K_9}{K_1} + \frac{2}{3} \frac{k_{24} + k_{2,10}}{K_1} \right) \right] w_{,xxxx} + \alpha^2 h^4 \left\{ k_{1,10} - \left[(k_{15} + k_{1,11}) \frac{K_{10}}{K_1} \right. \right. \\ \left. \left. + 2k_{1,11} \frac{k_{24} + k_{2,10}}{K_1} \right] - \left[(k_{19} + k_{1,12}) \frac{K_{11}}{K_2} + 2k_{1,12} \frac{k_{37} + k_{3,10}}{K_2} \right] \right\} w_{,xxyy} + \alpha^4 h^4 \left[\frac{1}{6}(k_{17} \right. \\ \left. + k_{1,10}) - (k_{19} + k_{1,12}) \left(\frac{K_{12}}{K_2} + \frac{2}{3} \frac{k_{37} + k_{3,10}}{K_2} \right) \right] w_{,yyyy} + h^6 \left[\frac{1}{180}(k_{14} + k_{1,10}) \right]$$

(Equation continued on next page)

APPENDIX D - Continued

$$\begin{aligned}
 & - (k_{15} + k_{1,11}) \left(\frac{1}{4} \frac{K_3^2}{K_1^2} + \frac{K_9}{6K_1} + \frac{1}{30} \frac{k_{24} + k_{2,10}}{K_1} \right) w_{,xxxxxxx} + \alpha^2 h^6 \left[\frac{1}{12} k_{1,10} \right. \\
 & - (k_{15} + k_{1,11}) \left(\frac{1}{4K_1^2} K_4^2 + \frac{K_{10}}{6K_1} \right) - k_{1,11} \left(\frac{K_9}{2K_1} + \frac{1}{3} \frac{k_{24} + k_{2,10}}{K_1} \right) - (k_{19} + k_{1,12}) \frac{K_6^2}{4K_2^2} \\
 & - k_{1,12} \left(\frac{K_{11}}{2K_2} + \frac{1}{6} \frac{k_{37} + k_{3,10}}{K_2} \right) \left. \right] w_{,xxxxxyy} + \alpha^4 h^6 \left[\frac{1}{12} k_{1,10} - (k_{15} + k_{1,11}) \frac{1}{4K_1^2} K_5^2 \right. \\
 & - k_{1,11} \left(\frac{K_{10}}{2K_1} + \frac{1}{6} \frac{k_{24} + k_{2,10}}{K_1} \right) - (k_{19} + k_{1,12}) \left(\frac{K_7^2}{4K_2^2} + \frac{K_{11}}{6K_2} \right) - k_{1,12} \left(\frac{K_{12}}{2K_2} \right. \\
 & \left. + \frac{1}{3} \frac{k_{37} + k_{3,10}}{K_2} \right) \left. \right] w_{,xyyyyyy} + \alpha^6 h^6 \left[\frac{1}{180} (k_{17} + k_{1,10}) - (k_{19} + k_{1,12}) \left(\frac{K_8^2}{4K_2^2} + \frac{K_{12}}{6K_2} \right. \right. \\
 & \left. \left. + \frac{1}{30} \frac{k_{37} + k_{3,10}}{K_2} \right) \right] w_{,yyyyyyy} + \dots = \frac{q\alpha^2 h^4}{D} \tag{D8}
 \end{aligned}$$

where

$$K_9 = 2(k_{24} + k_{2,10}) \left(\frac{1}{3} - \frac{k_{25} + k_{2,11}}{K_1} \right)$$

$$K_{10} = 2 \left[k_{2,10} - (k_{28} + k_{2,11}) \frac{k_{24} + k_{2,10}}{K_1} - 2k_{2,12} \frac{k_{37} + k_{3,10}}{K_2} \right]$$

$$K_{11} = 2 \left[k_{3,10} - (k_{36} + k_{3,12}) \frac{k_{37} + k_{3,10}}{K_2} - 2k_{3,11} \frac{k_{24} + k_{2,10}}{K_1} \right]$$

$$K_{12} = 2(k_{37} + k_{3,10}) \left(\frac{1}{3} - \frac{k_{39} + k_{3,12}}{K_2} \right)$$

(Equation continued on next page)

$$\left. \begin{aligned}
 K_3^2 &= 2(k_{24} + k_{2,10}) \left[(k_{25} + k_{2,11}) \left(2 \frac{k_{25} + k_{2,11}}{K_1} - 1 \right) + \frac{K_1}{15} \right] \\
 K_4^2 &= -4k_{2,11}(k_{24} + k_{2,10}) + \frac{4}{3} K_1 k_{2,10} - 2(k_{25} + k_{2,11})K_{10} - 2(k_{28} + k_{2,11})K_9 \\
 &\quad - 4 \frac{K_1}{K_2} k_{2,12} \left[K_{11} + \frac{2}{3} (k_{37} + k_{3,10}) \right] \\
 K_5^2 &= \frac{2}{3} K_1 k_{2,10} - 2(k_{28} + k_{2,11}) \left[K_{10} + \frac{1}{3} (k_{24} + k_{2,10}) \right] \\
 &\quad + 8 \frac{K_1}{K_2} (k_{37} + k_{3,10}) k_{2,12} \left(\frac{k_{39} + k_{3,12}}{K_2} - \frac{2}{3} \right) \\
 K_6^2 &= -2(k_{36} + k_{3,12}) \left[K_{11} + \frac{1}{3} (k_{37} + k_{3,10}) \right] + \frac{2}{3} K_2 k_{3,10} \\
 &\quad - 8 \frac{K_2}{K_1} (k_{24} + k_{2,10}) k_{3,11} \left(\frac{2}{3} - \frac{k_{25} + k_{2,11}}{K_1} \right) \\
 K_7^2 &= -2(k_{36} + k_{3,12})K_{12} - 2(k_{39} + k_{3,12})K_{11} - 4 \frac{K_2}{K_1} k_{3,11} \left[K_{10} + \frac{2}{3} (k_{24} + k_{2,10}) \right] \\
 &\quad - 4k_{3,12}(k_{37} + k_{3,10}) + \frac{4}{3} K_2 k_{3,10} \\
 K_8^2 &= 2(k_{37} + k_{3,10}) \left[(k_{39} + k_{3,12}) \left(2 \frac{k_{39} + k_{3,12}}{K_2} - 1 \right) + \frac{K_2}{15} \right]
 \end{aligned} \right\} \quad (D9)$$

Equation (D8) in terms of general stiffness coefficients represents the vertical equilibrium equation of a plate approximated by finite elements in terms of the displacement w , and equations (D5) and (D6) are the constraints between θ , φ , and w . Equations (D5), (D6), and (D8) can be used to investigate the convergence of the finite element equations at a typical node point when the stiffness properties of the element are given in the form of equation (D1).

APPENDIX E

COMPARISON OF FINITE DIFFERENCE AND FINITE ELEMENT APPROXIMATIONS

It is interesting to compare finite element approximations with the widely used central difference approximations to structural differential equations of equilibrium. While correlation is not obvious for all classes of problems some observations can be made.

One-Dimensional Extensional Bar

The governing equation for a one-dimensional bar subjected to a distributed inplane load p is

$$u_{,xx} + \frac{p}{EA} = 0 \quad (E1)$$

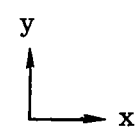
where the subscripts following the comma indicate differentiation with respect to the indicated variable. Application of central finite difference approximations to equation (E1) for unequal nodal spacing h and αh gives

$$\frac{2}{(1 + \alpha)h} \left(u_{i-1} - \frac{1 + \alpha}{\alpha} u_i + \frac{1}{\alpha} u_{i+1} \right) = \frac{p_i}{EA} \quad (E2)$$

Comparison of equation (E2) with the finite element equation approximated by segments of unequal length (eq. (3)) indicates that for this simple problem the finite difference and finite element equations are identical approximations.

Plane Stress

The governing equilibrium equation in the x -direction for a body in plane stress is given by equation (31). The central finite difference approximation to equation (31) is

$$\frac{1}{h^2} \left\{ \begin{array}{c} \frac{1 - \mu}{2\alpha^2} \\ \hline 1 \quad -2 \quad -\frac{1 - \mu}{\alpha^2} \quad 1 \\ \hline \frac{1 - \mu}{2\alpha^2} \end{array} \right\} u + \frac{1 + \mu}{8\alpha h^2} \left\{ \begin{array}{c} -1 \quad \quad \quad 1 \\ \hline \quad \quad \quad \quad \quad \\ \hline 1 \quad \quad \quad -1 \end{array} \right\} v + \frac{p_{x_i} \alpha h^2}{B} = 0 \quad (E3)$$


APPENDIX E – Continued

The corresponding finite element equation using rectangular elements and the same nodal spacing is

$$\frac{1}{h^2} \left\{ \begin{array}{c} \frac{1-\mu}{2\alpha^2} \\ \hline 1 \quad -2 \quad -\frac{1-\mu}{\alpha^2} \\ \hline \frac{1-\mu}{2\alpha^2} \end{array} \right\} u + c_1 \frac{1}{h^2 \alpha^2} \left\{ \begin{array}{c} 1 \quad -2 \quad 1 \\ \hline -2 \quad 4 \quad -2 \\ \hline 1 \quad -2 \quad 1 \end{array} \right\} u + \frac{1+\mu}{8\alpha h^2} \left\{ \begin{array}{c} -1 \quad 1 \\ \hline 1 \quad -1 \end{array} \right\} v + \frac{P_{X_i} \alpha h^2}{B} = 0 \quad (E4)$$

where c_1 takes the following values for the two finite models considered in this paper:

Linear stress model

$$c_1 = \frac{1-\mu}{8} + \frac{\alpha^2(2+\mu^2)}{12} \quad (E5)$$

Linear edge displacement model

$$c_1 = \frac{1-\mu}{12} + \frac{\alpha^2}{6} \quad (E6)$$

The Taylor series expansion of the finite element equations about the point i,j can be written as

$$u_{,xx} + \frac{1-\mu}{2} u_{,yy} + \frac{1+\mu}{2} v_{,xy} + \frac{h^2}{12} \left[u_{,xxxx} + \frac{\alpha^2(1-\mu^2)}{2} u_{,yyyy} + (1+\mu)v_{,xxxx} + \alpha^2(1+\mu)v_{,xyyy} \right] + h^2 c_1 u_{,xxyy} + \dots + \frac{P_X}{B} = 0 \quad (E7)$$

Study of equation (E7) shows that the finite element and finite difference equations for equation (31) are related by

$$E_X(u,v) = D_X(u,v) + c_1 h^2 \frac{\Delta^4 u}{\Delta x^2 \Delta y^2} \quad (E8)$$

where $E_X(u,v)$ and $D_X(u,v)$ are the element and difference operators, respectively, and where the central finite difference operator for $u_{,xxyy}$ is

$$\frac{\Delta^4 u}{\Delta x^2 \Delta y^2} = \frac{1}{\alpha^2 h^4} \left\{ \begin{array}{c} 1 \quad -2 \quad 1 \\ \hline -2 \quad 4 \quad -2 \\ \hline 1 \quad -2 \quad 1 \end{array} \right\} u \quad (E9)$$

APPENDIX E – Continued

A similar investigation of the y-direction equilibrium equation gives the relations between the element and difference equations for equation (32)

$$E_y(u,v) = D_y(u,v) + c_1 h^2 \frac{\Delta^4 v}{\Delta x^2 \Delta y^2} \quad (E10)$$

where E_y and D_y are the corresponding element and difference operators. Equations (E8) and (E10) suggest that any set of consistent finite element or finite difference operators for a rectangular mesh where the variables are the displacements at the nodes are related by

$$E_x(u,v)_{i,j} = D_x(u,v)_{i,j} + h^2 \left(\bar{c}_1 \frac{\Delta^4 u}{\Delta x^2 \Delta y^2} + \bar{c}_2 \frac{\Delta^4 v}{\Delta x^2 \Delta y^2} \right)_{i,j} \quad (E11)$$

$$E_y(u,v)_{i,j} = D_y(u,v)_{i,j} + h^2 \left(\bar{c}_3 \frac{\Delta^4 u}{\Delta x^2 \Delta y^2} + \bar{c}_4 \frac{\Delta^4 v}{\Delta x^2 \Delta y^2} \right)_{i,j} \quad (E12)$$

where the quantities \bar{c}_i are constants. Usually as a result of symmetry in assumptions on behavior of u and v these quantities \bar{c}_i will be related by

$$\left. \begin{aligned} \bar{c}_1 &= \bar{c}_4 \\ \bar{c}_2 &= \bar{c}_3 \end{aligned} \right\} \quad (E13)$$

If $\bar{c}_i = 0$, the element operator becomes the standard central finite difference operator.

Since these approximations all have the same error of order h^2 , the element and difference equations converge at the same rate. Thus the relative accuracy of the various approximations will depend on the problem solved. If the twist terms $u_{,xxyy}$ and $v_{,xxyy}$ are large for a problem, the finite element answers will be less accurate than the finite difference answers. For example consider the problem treated previously by finite element approximation, namely, a square plane stress plate subjected to an inplane harmonic loading in the y-direction. A solution to this same problem by central finite differences gives the errors resulting from the finite difference approximations ϵ_u and ϵ_v as

$$\epsilon_u = \frac{-h^2 \pi^2 m^2 n^2}{24a^2(1-\mu)(m^2+n^2)} (11 - 2\mu + 3\mu^2) \quad (E14)$$

APPENDIX E - Continued

$$\epsilon_v = - \frac{h^2 \pi^2}{6a^2(1-\mu)} \frac{-\frac{1-\mu}{2} m^8 + \frac{1+10\mu+\mu^2}{4} m^6 n^2 + \frac{3+23\mu+\mu^2-3\mu^3}{8} m^4 n^4 + \frac{-5+11\mu-3\mu^2-3\mu^3}{8} m^2 n^6 + \frac{-1+2\mu-\mu^2}{4} n^8}{m^6 + \frac{5-\mu}{2} m^4 n^2 + (2-\mu)m^2 n^4 + \frac{1-\mu}{2} n^6} \quad (E15)$$

The following table compares the error magnitude of the finite element results with finite difference results for $m = n$ and for Poisson's ratios $\mu = 0$ and 0.3 :

	$\mu = 0$		$\mu = 0.3$	
	$\epsilon_u N^2$	$\epsilon_v N^2$	$\epsilon_u N^2$	$\epsilon_v N^2$
Finite difference	-2.26	0.21	-3.13	-0.67
Linear stress	2.06	2.60	1.85	2.40
Linear edge displacement	1.44	2.26	1.15	1.97

The results indicate that neither the finite element nor the finite difference method is clearly superior for the approximate solution to plane stress problems.

Beam Element

When bending is introduced the correlation between finite difference and finite elements is more complex. This complexity is caused by the introduction of rotation variables at the nodes in the finite element procedure, whereas finite difference methods are not usually developed on that basis. Some correlation can however be made for the simple beam. Consider the beam equation

$$w^{iv} = \frac{q}{EI} \quad (E16)$$

The fourth derivative at a point i can be approximated by using data only at the points $i - 1$, i , and $i + 1$ by passing a fifth-degree polynomial through these three points and by expressing this polynomial in terms of w_i and θ_i , where θ_i is the derivative of the function at the node point

$$\begin{aligned} w(x) = & w_i + \theta_i x + \left(\frac{w_{i-1} - 2w_i + w_{i+1}}{h^2} + \frac{\theta_{i-1} - \theta_{i+1}}{4h} \right) x^2 \\ & + \left(\frac{-5w_{i-1} + 5w_{i+1}}{4h^3} - \frac{\theta_{i-1} + 8\theta_i + \theta_{i+1}}{4h^2} \right) x^3 + \left(\frac{-w_{i-1} + 2w_i - w_{i+1}}{2h^4} - \frac{\theta_{i-1} - \theta_{i+1}}{4h^3} \right) x^4 \\ & + \left(\frac{3w_{i-1} - 3w_{i+1}}{4h^5} + \frac{\theta_{i-1} + 4\theta_i + \theta_{i+1}}{4h^4} \right) x^5 \end{aligned} \quad (E17)$$

APPENDIX E – Continued

Differentiating $w(x)$ four times and evaluating it at point i gives

$$w^{iv} = 12 \left(\frac{-w_{i-1} + 2w_i - w_{i+1}}{h^4} + \frac{-\theta_{i-1} + \theta_{i+1}}{2h^3} \right) \quad (E18)$$

Substitution of equation (E18) into equation (E16) gives a finite difference equation which is identical with the finite element equation for vertical equilibrium. There remains however to relate the moment equilibrium finite element equation to finite differences. This is done by recognizing that the moment finite element equation is a constraint between slope and displacement variable. This side constraint between these variables can be written exactly as

$$w_{i+1} = w_{i-1} + \int_{i-1}^{i+1} \theta \, dx \quad (E19)$$

Approximating the integral in equation (E19) by Simpson's one-third rule gives

$$w_{i+1} = w_{i-1} + \frac{h}{3} (\theta_{i-1} + 4\theta_i + \theta_{i+1}) \quad (E20)$$

Comparisons show that equation (E19) is identical with the moment equilibrium finite element equation. The implicit use of the Simpson's integration formula indicates why the finite element approximation has greater accuracy and a higher order of error, namely, because the error in Simpson's rule is of order h^5 , whereas central difference approximations are of order h^2 . Some comparison of the relative accuracies of the standard central difference and finite element approximations can be determined by considering the simply supported beam example subjected to a harmonic loading. The central difference approximation to w^{iv} is

$$w_i^{iv} = \frac{1}{h^4} (w_{i-2} - 4w_{i-1} + 6w_i - 4w_{i+1} + w_{i+2}) \quad (E21)$$

which when expanded in a Taylor series and applied to the harmonic load example problem is

$$w^{iv} + \frac{h^2 w^{vi}}{6} + \dots = \frac{q}{EI} \sin \frac{m\pi x}{L} \quad (E22)$$

Solution to equation (E22) is

$$w = w_{ex}(1 + \epsilon_d) \quad (E23)$$

where w_{ex} is the exact solution and ϵ_d the error due to the finite difference approximations

$$\epsilon_d = \frac{h^2}{6} \left(\frac{m\pi}{L} \right)^2 = \frac{1}{N_d^2} \frac{\pi^2}{6} \quad (E24)$$

APPENDIX E - Concluded

where N_d is the number of finite difference segments. Note that the finite difference error is proportional to $1/N_d^2$ whereas the finite element error is proportional to $1/N^4$. (See eq. (19).) Thus the finite element approximation is more accurate than the finite difference approximation for the same element size. On the other hand, the element equations lead to twice as many variables as the difference equations. For a 1-percent error in this example approximately two finite element segments and 13 finite difference segments are required.

REFERENCES

1. Clough, Ray W.; and Tocher, James L.: Finite Element Stiffness Matrices for Analysis of Plate Bending. Matrix Methods in Structural Mechanics, AFFDL-TR-66-80, U.S. Air Force, [1965], pp. 515-545. (Available from DDC as AD 646 300.)
2. Walz, Joseph E.; Fulton, Robert E.; and Cyrus, Nancy Jane: Accuracy and Convergence of Finite Element Approximations. Paper presented at the Air Force Second Conference on Matrix Methods in Structural Mechanics (Wright-Patterson AFB), Oct. 15-17, 1968.
3. Fulton, Robert E.; Eppink, Richard T.; and Walz, Joseph E.: The Accuracy of Finite Element Methods in Continuum Problems. Paper presented at Fifth U.S. National Congress of Applied Mechanics (Minneapolis, Minn.), June 14-17, 1966.
4. Cyrus, Nancy Jane; and Fulton, Robert E.: Finite Difference Accuracy in Structural Analysis. J. Struct. Div., Amer. Soc. Civil Eng., vol. 92, no. ST6, Dec. 1966, pp. 459-471.
5. Cyrus, Nancy Jane; and Fulton, Robert E.: Accuracy Study of Finite Difference Methods. NASA TN D-4372, 1968.
6. Moulton, Forest Ray: Differential Equations. Macmillan Co., 1930.
7. Timoshenko, S.; and Woinowsky-Krieger, S.: Theory of Plates and Shells. Second ed., McGraw-Hill Book Co., Inc., 1959.
8. Langhaar, Henry L.: Energy Methods in Applied Mechanics. John Wiley & Sons, Inc., c.1962.
9. Flügge, Wilhelm: Stresses in Shells. Second printing, Springer-Verlag (Berlin), 1962.
10. Koiter, W. T.: A Consistent First Approximation in the General Theory of Thin Elastic Shells. The Theory of Thin Elastic Shells, W. T. Koiter, ed., Interscience Publ., Inc., 1960, pp. 12-13.
11. Canton, Gilles; and Clough, Ray W.: A Curved, Cylindrical-Shell, Finite Element. AIAA J., vol. 6, no. 6, June 1968, pp. 1057-1062.
12. Gallagher, Richard H.: A Correlation Study of Methods of Matrix Structural Analysis. AGARDograph 69, Pergamon Press, Inc., 1964.
13. Turner, M. J.; Clough, R. W.; Martin, H. C.; and Topp, L. J.: Stiffness and Deflection Analysis of Complex Structures. J. Aeron. Sci., vol. 23, no. 9, Sept. 1956, pp. 805-823, 854.

14. Papenfuss, Bruce Willes: Lateral Plate Deflection by Stiffness Matrix Methods With Application to a Marquee. M.S. Thesis, Univ. of Washington, 1959.
15. Melosh, Robert J.: A Stiffness Matrix for the Analysis of Thin Plates in Bending. J. Aerosp. Sci., vol. 28, no. 1, Jan. 1961, pp. 34-42, 64.
16. Adini, Ari; and Clough, Ray W.: Analysis of Plate Bending by the Finite Element Method. Grant NSF-G7337, Univ. of California (Berkeley), Mar. 1960.
17. Melosh, Robert J.: Basis for Derivation of Matrices for the Direct Stiffness Method. AIAA J., vol. 1, no. 7, July 1963, pp. 1631-1637.

TABLE I.- FINITE ELEMENT DISCRETIZATION ERROR

(a) One-dimensional elements

Element	Nodal variables	Governing differential equations	Error terms (appearing in left-hand side of equations)
Bar:			
Unequal segments	$\{u\}$	$u'' + \frac{p}{EA} = 0$	$-\frac{h}{3}(1 - \alpha)u''' + \frac{h^2}{12}\left(\frac{1 + \alpha^3}{1 + \alpha}\right)u^{iv} + \dots$
Equal segments	$\{u\}$	$u'' + \frac{p}{EA} = 0$	$+\frac{h^2}{12}u^{iv} + \dots$
Beam			
	$\left\{ \begin{matrix} w \\ \theta \end{matrix} \right\}$	$w^{iv} = \frac{q}{EI}$ $\theta = w'$	$-\frac{h^4}{720}w^{viii} + \dots$ $+\frac{h^4}{180}w^v + \dots$
Arch:			
Straight segments	$\left\{ \begin{matrix} u \\ w \\ \theta \end{matrix} \right\}$	$EA\left(-u'' + \frac{w'}{R}\right) - \frac{EI}{R}\left(w'''' + \frac{u''}{R}\right) - p = 0$	$+O(h^2)$
		$EI\left(w^{iv} + \frac{u''''}{R}\right) + EA\left(-\frac{u'}{R} + \frac{w}{R^2}\right) - q = 0$	$+O(h^2)$
		$\theta = w' + \frac{u}{R}$	$+O(h^2)$
Curved segments	$\left\{ \begin{matrix} u \\ w \\ \theta \end{matrix} \right\}$	$EA\left(-u'' + \frac{w'}{R}\right) - p = 0$	$+h^2EA \frac{1}{12}\left(-u^{iv} + \frac{w''''}{R}\right)$
		$EI\left(w^{iv} + 2\frac{w'''}{R^2} + \frac{w}{R^4}\right) + EA\left(-\frac{u'}{R} + \frac{w}{R^2}\right) - q = 0$ $\theta = w' + \frac{u}{R}$	$-h^2EA\left(\frac{u''''}{12R}\right)$ $+O(h^4)$

TABLE I.- FINITE ELEMENT DISCRETIZATION ERROR - Continued

(b) Plane stress elements

Variables

$$\begin{Bmatrix} u \\ v \end{Bmatrix}$$

Governing differential equations

$$(1) \quad u_{,xx} + \frac{1-\mu}{2} u_{,yy} + \frac{1+\mu}{2} v_{,xy} + \frac{P_x}{B} = 0$$

$$(2) \quad \frac{1+\mu}{2} u_{,xy} + \frac{1-\mu}{2} v_{,xx} + v_{,yy} + \frac{P_y}{B} = 0$$

Element	Equation	Error terms (appearing in left-hand side of equations)
Rectangle, linear stress distribution	(1)	$+ \frac{h^2}{12} \left\{ u_{,xxxx} + \left[\frac{3}{2}(1-\mu) + \alpha^2(2+\mu^2) \right] u_{,xxyy} + \frac{1-\mu}{2} \alpha^2 u_{,yyyy} + (1+\mu)v_{,xxxy} + (1+\mu)\alpha^2 v_{,xyyy} \right\} + \dots$
	(2)	$+ \frac{h^2}{12} \left\{ (1+\mu)u_{,xxxy} + (1+\mu)\alpha^2 u_{,xyyy} + \frac{1-\mu}{2} v_{,xxxx} + \left[\frac{3}{2}\alpha^2(1-\mu) + (2+\mu^2) \right] v_{,xxyy} + \alpha^2 v_{,yyyy} \right\} + \dots$
Rectangle, linear edge displacement	(1)	$+ \frac{h^2}{12} \left\{ u_{,xxxx} + \left[(1-\mu) + 2\alpha^2 \right] u_{,xxyy} + \frac{1-\mu}{2} \alpha^2 u_{,yyyy} + (1+\mu)v_{,xxxy} + (1+\mu)\alpha^2 v_{,xyyy} \right\} + \dots$
	(2)	$+ \frac{h^2}{12} \left\{ (1+\mu)u_{,xxxy} + (1+\mu)\alpha^2 u_{,xyyy} + \frac{1-\mu}{2} v_{,xxxx} + \left[\alpha^2(1-\mu) + 2 \right] v_{,xxyy} + \alpha^2 v_{,yyyy} \right\} + \dots$
Right triangle, pattern A	(1)	$+ \frac{h^2}{12} \left[u_{,xxxx} + \alpha^2 \left(\frac{1-\mu}{2} \right) u_{,yyyy} + 2\alpha v_{,xxxy} + 3\alpha^2 v_{,xxyy} + 2\alpha^3 v_{,xyyy} \right] + \dots$
	(2)	$+ \frac{h^2}{12} \left[2\alpha u_{,xxxy} + 3\alpha^2 u_{,xxyy} + 2\alpha^3 u_{,xyyy} + \left(\frac{1-\mu}{2} \right) v_{,xxxx} + \alpha^2 v_{,yyyy} \right] + \dots$
Right triangle, pattern B	(1)	$- \frac{1+\mu}{2} v_{,xy} + \frac{h^2}{12} \left(u_{,xxxx} + \frac{1-\mu}{2} \alpha^2 u_{,yyyy} \right) + \dots$
	(2)	$- \frac{1+\mu}{2} u_{,xy} + \frac{h^2}{12} \left(\frac{1-\mu}{2} v_{,xxxx} + \alpha^2 v_{,yyyy} \right) + \dots$
Right triangle, pattern C	(1)	$+ \frac{1+\mu}{2} v_{,xy} + \frac{h^2}{12} \left[u_{,xxxx} + \frac{1-\mu}{2} \alpha^2 u_{,yyyy} + 2(1+\mu)v_{,xxxy} + 2(1+\mu)\alpha^2 v_{,xxyy} \right] + \dots$
	(2)	$+ \frac{1+\mu}{2} u_{,xy} + \frac{h^2}{12} \left[2(1+\mu)u_{,xxxy} + 2(1+\mu)\alpha^2 u_{,xxyy} + \frac{1-\mu}{2} v_{,xxxx} + \alpha^2 v_{,yyyy} \right] + \dots$
Equilateral triangle	(1)	$+ h^2 \left(\frac{7+\mu}{96} u_{,xxxx} + \frac{1+\mu}{16} u_{,xxyy} + \frac{1-\mu}{32} u_{,yyyy} + \frac{1+\mu}{48} v_{,xxxy} + \frac{1+\mu}{16} v_{,xxyy} \right) + \dots$
	(2)	$+ h^2 \left(\frac{1+\mu}{16} u_{,xxxy} + \frac{1+\mu}{48} u_{,xxyy} + \frac{1-\mu}{32} v_{,xxxx} + \frac{1+\mu}{16} v_{,xxyy} + \frac{7+\mu}{96} v_{,yyyy} \right) + \dots$

TABLE I.- FINITE ELEMENT DISCRETIZATION ERROR – Concluded

(c) Rectangular plate bending elements

Variables

$$\begin{Bmatrix} w \\ \theta \\ \varphi \end{Bmatrix}$$

Governing differential equations

(1) $\nabla^4 w = \frac{q}{D}$

(2) $\theta = w_{,x}$

(3) $\varphi = w_{,y}$

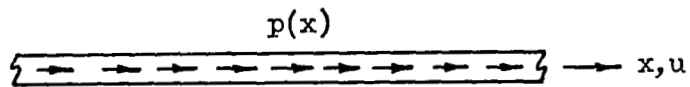
Element	Equation	Error terms (appearing in left-hand side of equations)
Melosh	(1)	$+ h^2 \left\{ \left(\frac{1}{6} - \frac{\mu}{12} + \frac{\alpha^2 \mu^2}{48} \right) w_{,xxxxxyy} + \left[\alpha^2 \left(\frac{1}{6} - \frac{\mu}{12} \right) + \frac{\mu^2}{48} \right] w_{,xxyyyyy} \right\} + \dots$
	(2)	$+ O(h^2)$
	(3)	$+ O(h^2)$
ACM	(1)	$+ h^2 \left[\frac{1}{6} (\alpha^2 + \mu) w_{,xxxxxyy} + \frac{1}{6} (1 + \mu \alpha^2) w_{,xxyyyyy} \right] + \dots$
	(2)	$+ O(h^4)$
	(3)	$+ O(h^4)$
Papenfuss	(1)	$+ \left(\frac{2}{35} \alpha^2 + \frac{2}{35 \alpha^2} + \frac{2}{25} \right) w_{,xxyy} + h^2 \left[\left(\frac{\alpha^6}{3675} + \frac{2}{2625} \alpha^4 + \frac{274}{91875} \alpha^2 - \frac{61}{2625} - \frac{146}{3675 \alpha^2} \right) w_{,xxxxxyy} \right.$ $\left. + \alpha^2 \left(\frac{1}{3675 \alpha^6} + \frac{2}{2625 \alpha^4} + \frac{274}{91875 \alpha^2} - \frac{61}{2625} - \frac{146 \alpha^2}{3675} \right) w_{,xxyyyyy} \right] + \dots$
	(2)	$+ O(h^2)$
	(3)	$+ O(h^2)$

TABLE II.- ERROR TERMS FOR HARMONIC RESPONSE EXAMPLES

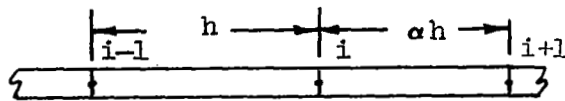
Element	Error terms
<p>Bar:</p> $p = p_0 \sin \frac{m\pi x}{L}$ $u = u_{ex}(1 + \epsilon)$ $u_{ex} = \frac{p_0}{EA} \left(\frac{L}{m\pi}\right)^2 \sin \frac{m\pi x}{L}$ $\omega^2 = \omega_{ex}^2(1 - \epsilon)$ $\omega_{ex}^2 = \frac{EA}{m} \left(\frac{m\pi}{L}\right)^2$	$\epsilon = \frac{\pi^2}{12N^2} \quad \left(N = \frac{L}{mh}\right)$
<p>Beam:</p> $q = q_0 \sin \frac{m\pi x}{L}$ $w = w_{ex}(1 + \epsilon)$ $w_{ex} = \frac{q_0}{EI} \left(\frac{L}{m\pi}\right)^4 \sin \frac{m\pi x}{L}$ $\omega^2 = \omega_{ex}^2(1 - \epsilon)$ $\omega_{ex}^2 = \frac{EI}{m} \left(\frac{m\pi}{L}\right)^4$	$\epsilon = \frac{\pi^4}{720N^4}$
<p>Arch:</p> $p = 0 \quad q = q_0 \sin \frac{mx}{R}$ <p>Curved segments:</p> $u = u_{ex}(1 + \epsilon_u)$ $w = w_{ex}(1 + \epsilon_w)$ $u_{ex} = \frac{-q_0 R^4}{EI m(m^2 - 1)^2} \cos \frac{mx}{R}$ $w_{ex} = \frac{q_0 R^4}{EI(m^2 - 1)^2} \sin \frac{mx}{R}$ <p>Straight segments:</p> $u = \bar{u}_{ex}(1 + \epsilon_{\bar{u}})$ $w = \bar{w}_{ex}(1 + \epsilon_{\bar{w}})$ $\bar{u}_{ex} = u_{ex} \left[1 + m^2 \left(\frac{\rho}{R}\right)^2 \right]$ $\bar{w}_{ex} = w_{ex} \left[1 + \left(\frac{\rho}{R}\right)^2 \right]$	<p>Curved segments:</p> $\epsilon_u = - \frac{\pi^2}{12N^2(m^2 - 1)^2 \left(\frac{\rho}{R}\right)^2}$ $\epsilon_w = - \frac{\pi^2}{12N^2(m^2 - 1)^2 \left(\frac{\rho}{R}\right)^2} \quad \left(N = \frac{\pi R}{mh}\right)$ <p>Straight segments:</p> $\epsilon_{\bar{u}} = 0 \left(\frac{1}{N^2}\right)$ $\epsilon_{\bar{w}} = 0 \left(\frac{1}{N^2}\right)$

TABLE II. - ERROR TERMS FOR HARMONIC RESPONSE EXAMPLES - Concluded

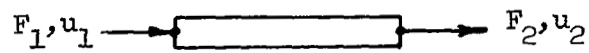
Element	Error terms
Plane stress rectangle:	Linear stress distribution:
$p_x = 0$	$\epsilon_u = \frac{h^2 \pi^2 m^2 n^2 (5 - 2\mu + \mu^2)}{12a^2 (m^2 + n^2)}$
$p_y = p_0 \sin \frac{m\pi x}{a} \sin \frac{n\pi y}{a}$	$\epsilon_v = \frac{h^2 \pi^2}{6a^2 (1 - \mu)} \frac{\frac{1 - \mu}{2} m^8 + \frac{13 - 16\mu + 3\mu^2}{4} m^6 n^2 + \frac{16 - 26\mu + 11\mu^2 - 2\mu^3 + \mu^4}{4} m^4 n^4 + \frac{6 - 14\mu + 9\mu^2 - 2\mu^3 + \mu^4}{4} m^2 n^6 + \left(\frac{1 - \mu}{2}\right)^2 n^8}{m^6 + \frac{5 - \mu}{2} m^4 n^2 + (2 - \mu) m^2 n^4 + \frac{1 - \mu}{2} n^6}$
$u = u_{ex}(1 + \epsilon_u)$	Linear edge displacement:
$v = v_{ex}(1 + \epsilon_v)$	$\epsilon_u = \frac{h^2 \pi^2 m^2 n^2 (7 - 10\mu - \mu^2)}{24a^2 (m^2 + n^2) (1 - \mu)}$
$u_{ex} = \frac{p_0 a^2 (1 + \mu) mn}{B\pi^2 (1 - \mu) (m^2 + n^2)^2} \cos \frac{m\pi x}{a} \cos \frac{n\pi y}{a}$	$\epsilon_v = \frac{h^2 \pi^2}{6a^2 (1 - \mu)} \frac{\frac{1 - \mu}{2} m^8 + \frac{11 - 14\mu - \mu^2}{4} m^6 n^2 + \frac{27 - 45\mu + 9\mu^2 + \mu^3}{8} m^4 n^4 + \frac{11 - 25\mu + 13\mu^2 + \mu^3}{8} m^2 n^6 + \left(\frac{1 - \mu}{2}\right)^2 n^8}{m^6 + \frac{5 - \mu}{2} m^4 n^2 + (2 - \mu) m^2 n^4 + \frac{1 - \mu}{2} n^6}$
$v_{ex} = \frac{2p_0 a^2 \left(m^2 + \frac{1 - \mu}{2} n^2\right)}{B\pi^2 (1 - \mu) (m^2 + n^2)^2} \sin \frac{m\pi x}{a} \sin \frac{n\pi y}{a}$	
Rectangular plate:	Melosh:
$q = q_0 \sin \frac{m\pi x}{a} \sin \frac{n\pi y}{a}$	$\epsilon_1 = \epsilon_2 = \frac{h^2 \pi^2}{a^2} \left(\frac{1}{6} - \frac{\mu}{12} + \frac{\mu^2}{48}\right) \frac{m^2 n^2}{m^2 + n^2}$
$w = w_{ex}(1 + \epsilon_1)$	ACM:
$w_{ex} = \frac{q_0 a^4}{D\pi^4 (m^2 + n^2)^2} \sin \frac{m\pi x}{a} \sin \frac{n\pi y}{a}$	$\epsilon_1 = \epsilon_2 = \frac{h^2 \pi^2}{a^2} \left(\frac{1 + \mu}{6}\right) \frac{m^2 n^2}{m^2 + n^2}$
$\omega^2 = \omega_{ex}^2 (1 - \epsilon_2)$	Papenfuss:
$\omega_{ex}^2 = \frac{D\pi^4 (m^2 + n^2)^2}{\bar{m} a^4}$	$\epsilon_1 = \frac{-m^2 n^2}{(m^2 + n^2)^2 + \frac{34}{175} m^2 n^2} \left\{ \frac{34}{175} + \frac{5416 h^2 \pi^2 (m^2 + n^2)^3}{91\,875 a^2 \left[(m^2 + n^2)^2 + \frac{34}{175} m^2 n^2 \right]} \right\}$
	$\epsilon_2 = \frac{-m^2 n^2}{m^2 + n^2} \left[\frac{34}{175 (m^2 + n^2)} + \frac{5416 h^2 \pi^2}{91\,875 a^2} \right]$



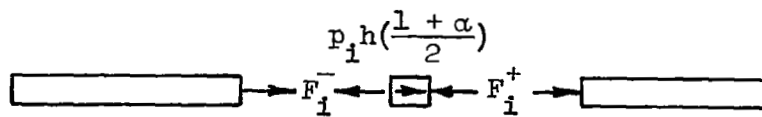
(a) Continuous bar.



(b) Approximation of continuous bar by finite elements.

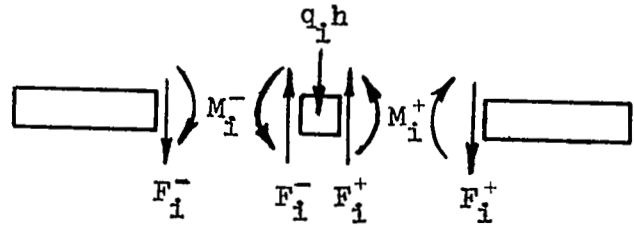
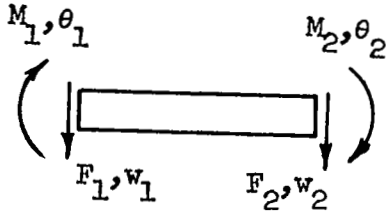
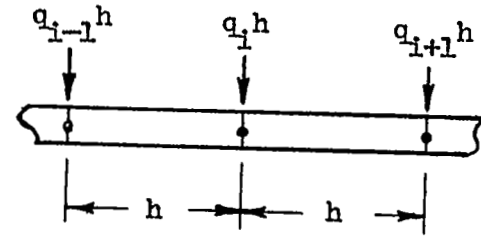
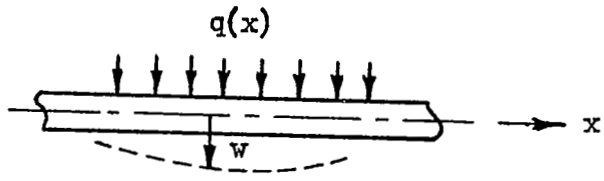


(c) Forces and displacements in bar finite elements.



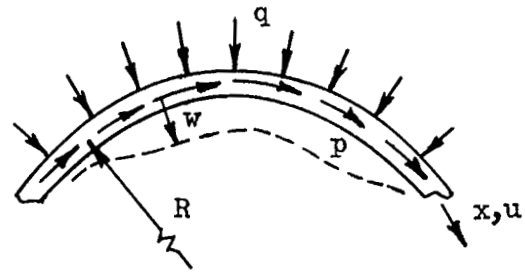
(d) Equilibrium at i th grid point in finite element assemblage.

Figure 1.- One-dimensional bar and its finite element representation.

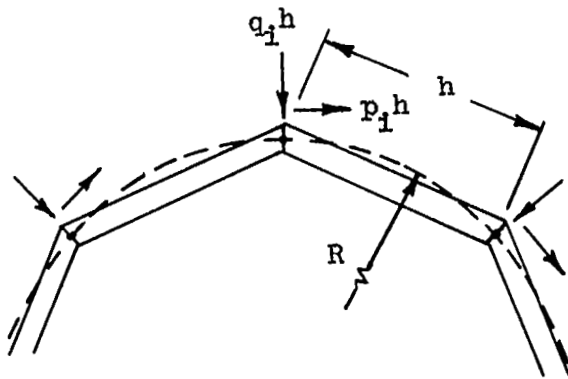


Equilibrium at i^{th} node

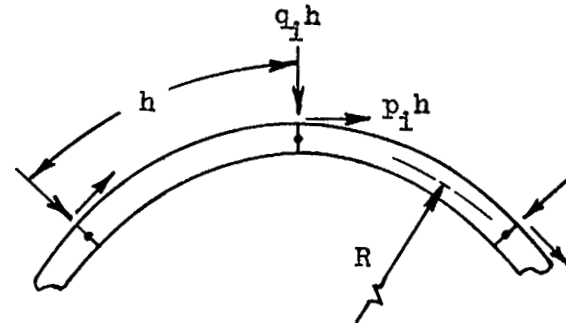
Figure 2.- Beam element.



Continuous arch structure

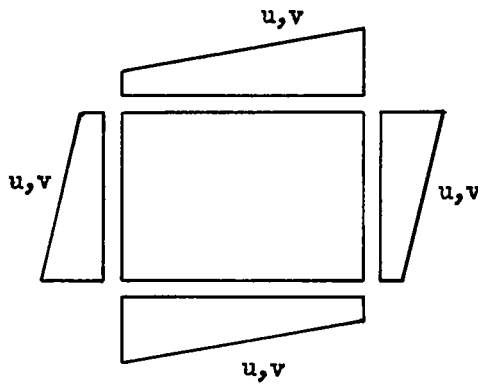
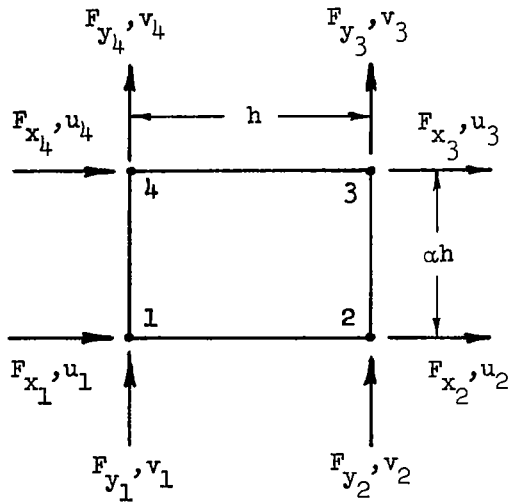
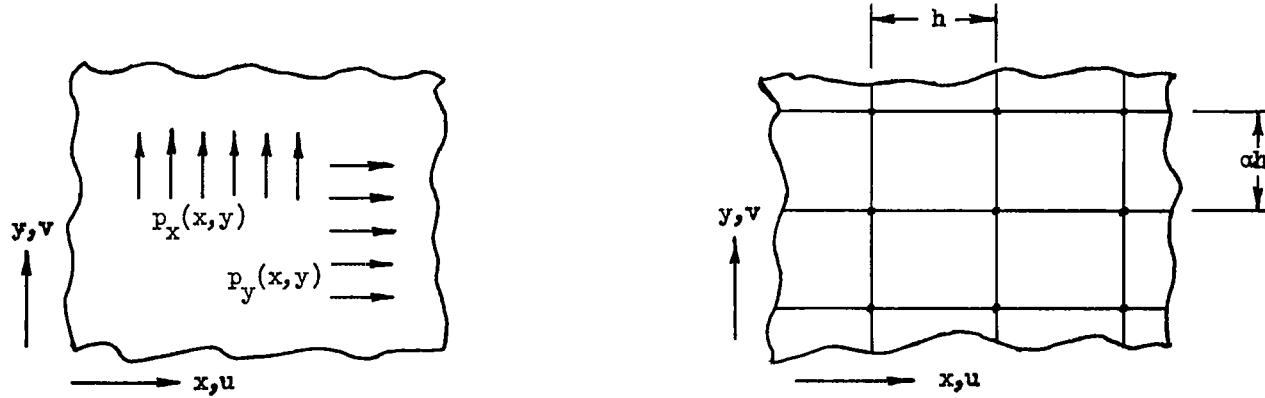


Straight element approximation

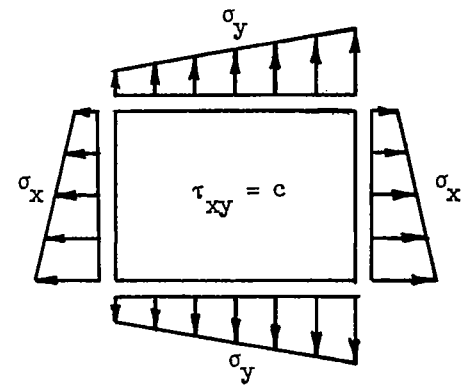


Curved element approximation

Figure 3.- Arch approximated by straight and curved elements.



Linear edge displacement model



Linear stress model

Figure 4.- Plane stress element.

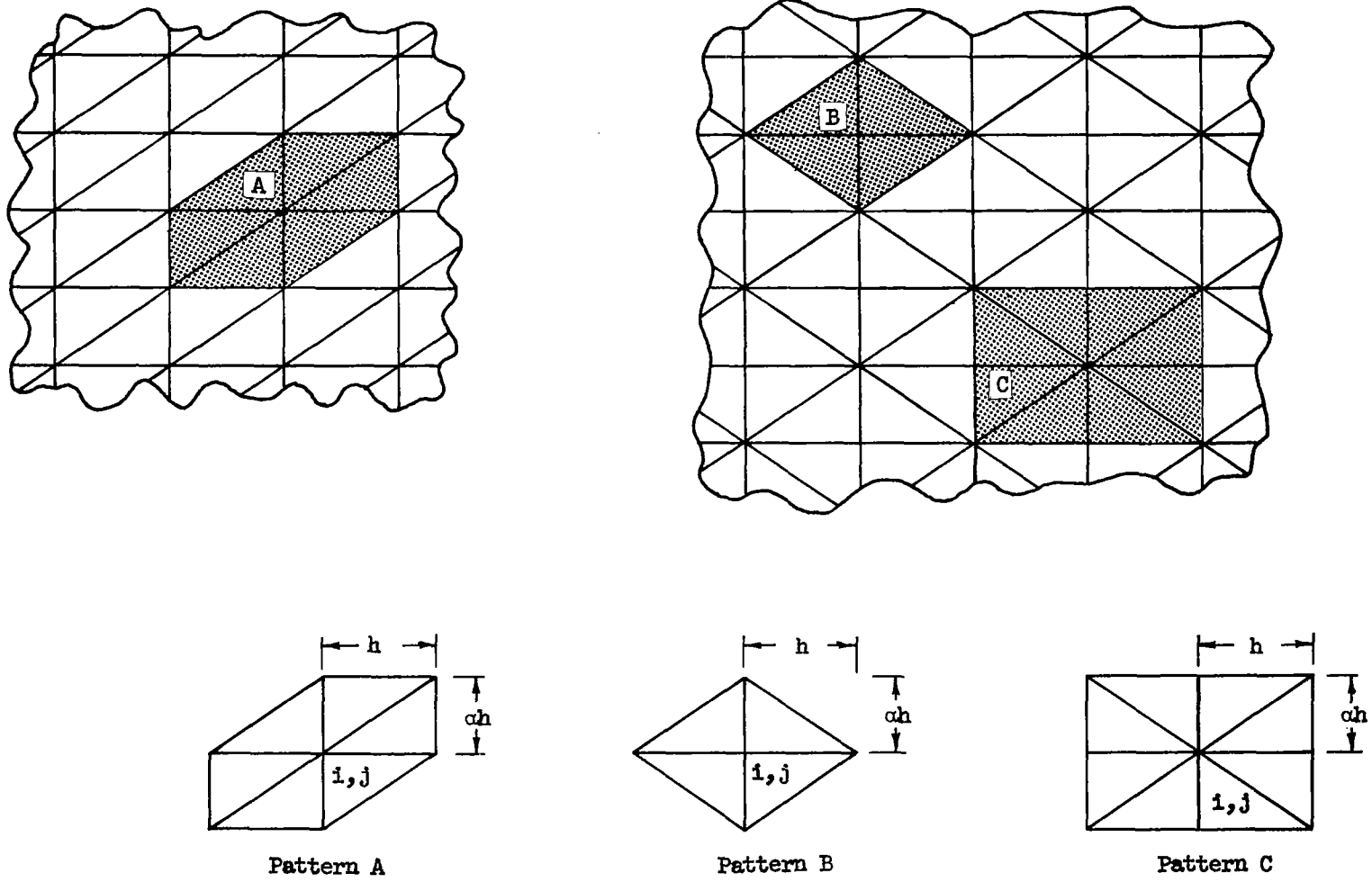


Figure 5.- Triangular finite element patterns.

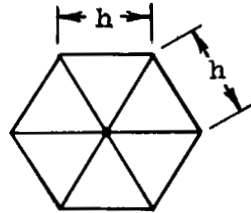
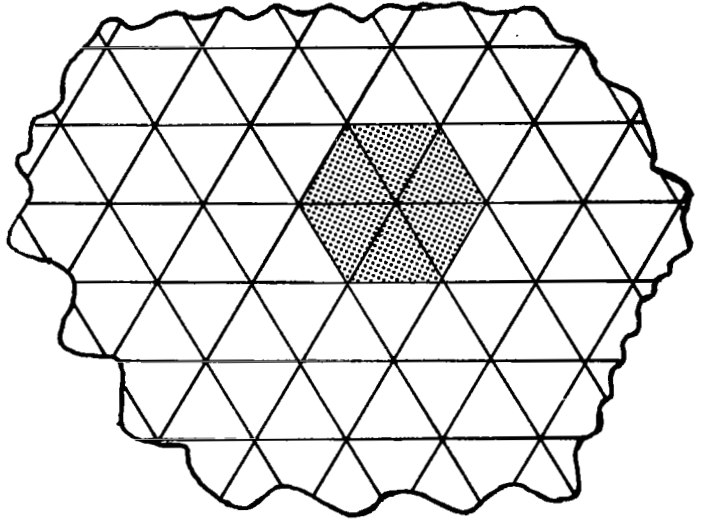


Figure 6.- Equilateral triangular finite element pattern.

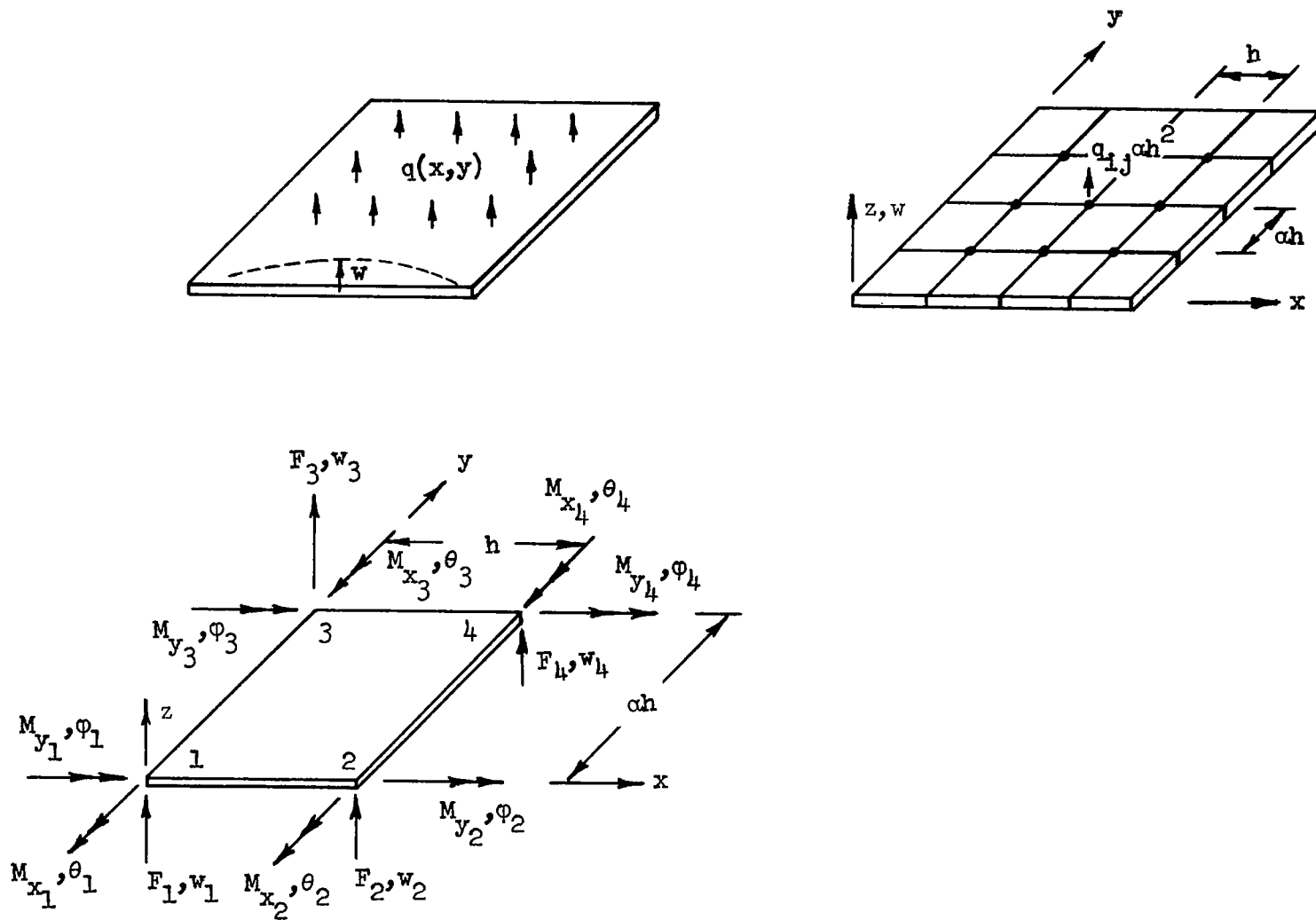


Figure 7.- Plate bending element.

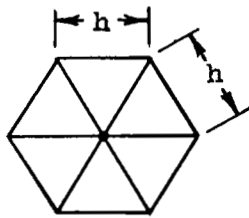
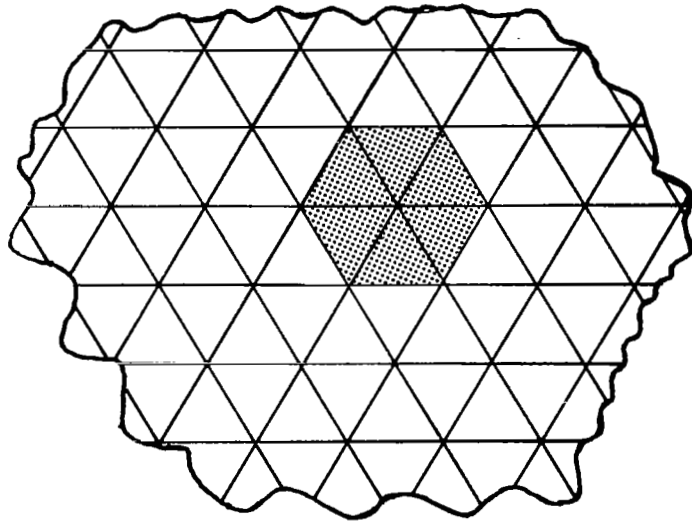


Figure 6.- Equilateral triangular finite element pattern.

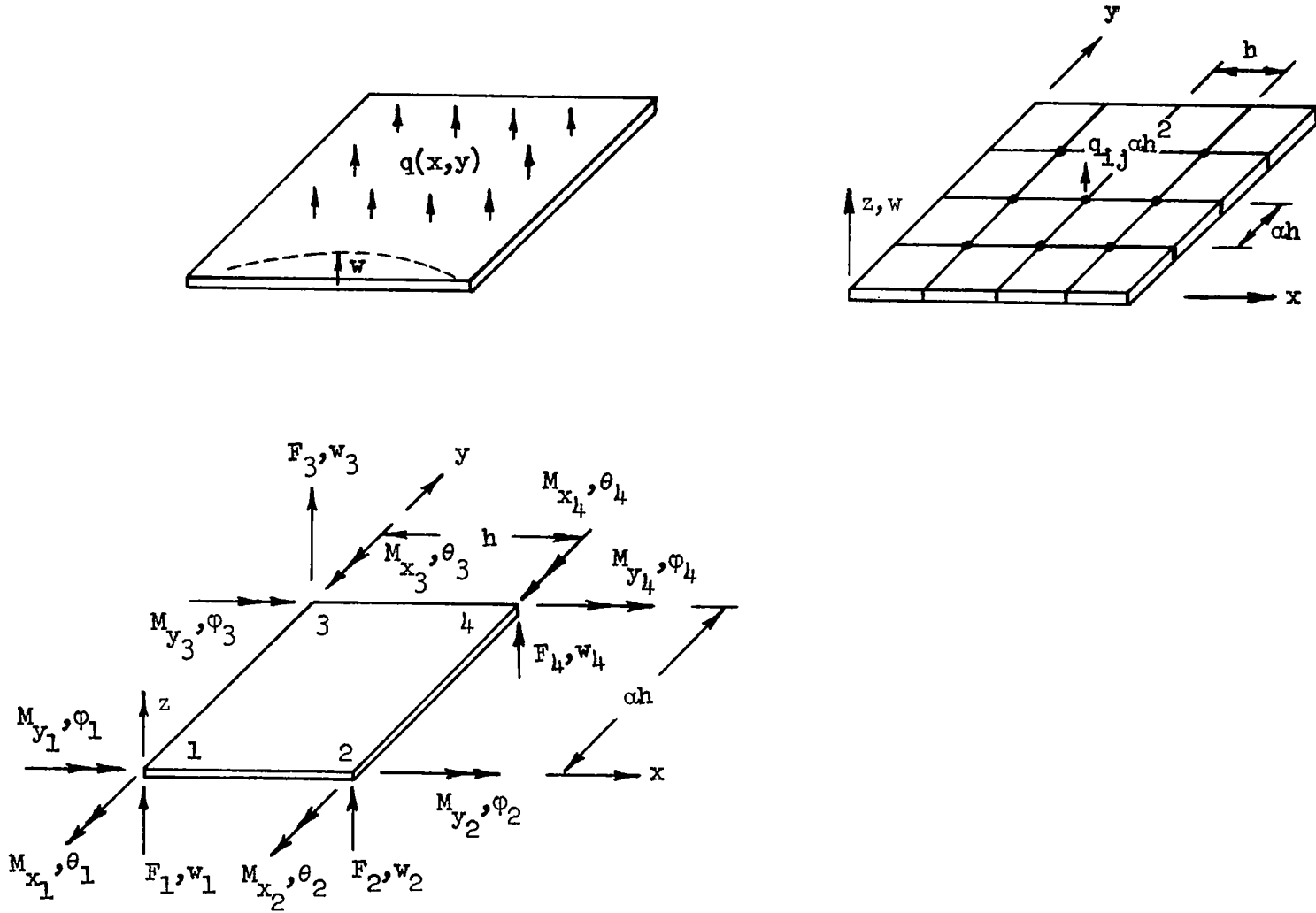


Figure 7.- Plate bending element.